

# ONE-DIMENSIONAL GAS DYNAMICS IN NITROUS OXIDE ROCKET SYSTEMS

A Thesis

by

EMILIO JOSE JIMENEZ

Submitted to the Graduate and Professional School of  
Texas A&M University  
in partial fulfillment of the requirements for the degree of  
MASTER OF SCIENCE

Chair of Committee, Adonios N. Karpetis  
Committee Members, Diego Donzis  
Eric L. Petersen  
Head of Department, Ivett Leyva

August 2022

Major Subject: Aerospace Engineering

Copyright 2022 Emilio Jose Jimenez

## ABSTRACT

Liquid and hybrid rocket systems that utilize high-pressure liquid nitrous oxide ( $N_2O$ ) are susceptible to accidental decompression. These very rare events have catastrophic potential and have led to loss of human life in the past. Traditional thinking considers those events as driven by catalytic chemical decomposition reactions; the objective of this work is to examine such events in the light of BLEVE (Boiling Liquid Expanding Vapor Explosion). The static picture of BLEVE will be described here as a metastable phase transition between liquid and vapor phases, using Clausius II thermodynamics (statics) to describe the retrograde behavior of the fluid. The dynamics of a hypothetical BLEVE process inside nitrous rocket-propellant tanks will also be examined using 1-D gas dynamics, and specifically by considering three 'canonical' flows and their combinations: Area variation, Fanno friction flow, and Rayleigh heat addition.

This thesis will provide an outline of Clausius II and how it was applied to various flows through the use of a 1D model coded in Python [5]. The results obtained from this coded model will be plotted and explained in order to either validate or give further work ideas to the theory initially provided.

## DEDICATION

To my parents, for their continued love and support of all my endeavors.

And to all my friends that have helped me through this degree.

## ACKNOWLEDGMENTS

I would like to thank the Texas A&M Department of Aerospace Engineering and College of Engineering for everything that I have learned in both my undergraduate and graduate education. Special thanks to Dr. Adonios Karpetis, Dr. Diego Donzis, and Dr. Eric Petersen for carefully reviewing this material.

## CONTRIBUTORS AND FUNDING SOURCES

### **Contributors**

This work was supported by a thesis committee consisting of Professor Adonios Karpelis [advisor] and Professor Diego Donzis of the Department of Aerospace Engineering, and Professor Eric Petersen of the Department of Mechanical Engineering.

All work conducted for the thesis was completed by the student independently.

### **Funding Sources**

Financial support by Texas A&M 02-247040 is gratefully acknowledged.

## NOMENCLATURE

$A_c$	Cross-sectional area ( $m^2$ )
$E$	Internal Energy ( $J$ )
$e$	Specific internal energy ( $J/kg$ )
$h$	Specific enthalpy ( $J/kg$ )
$m$	Mass ( $kg$ )
$p$	Pressure ( $Pa$ )
$\rho$	Density ( $kg/(m^3)$ )
$Q$	Heat transfer ( $J$ )
$\bar{R}$	Universal gas constant ( $8.314J/(mol * K)$ )
$s$	Specific Entropy ( $J/(K * kg)$ )
$T$	Temperature ( $K$ )
$t$	Time ( $s$ )
$u$	Velocity along x ( $m/s$ )
$v$	Specific volume ( $m^3/kg$ )
$\mathbf{V}$	Velocity vector ( $m/s$ )
$W$	Work ( $J$ )

# TABLE OF CONTENTS

	Page
ABSTRACT .....	ii
DEDICATION .....	iii
ACKNOWLEDGMENTS .....	iv
CONTRIBUTORS AND FUNDING SOURCES .....	v
NOMENCLATURE .....	vi
TABLE OF CONTENTS .....	vii
LIST OF FIGURES .....	ix
CHAPTER I INTRODUCTION .....	1
CHAPTER II METASTABILITY AND PHASE CHANGE .....	3
Metastability .....	3
Phase Change .....	4
Superheated Liquid .....	7
CHAPTER III MODELING METASTABILITY .....	9
Equations of State .....	9
Clausius II Equation of State .....	9
Clausius II Liquid-Vapor Coexistence .....	12
Maxwell Construction .....	12
Application of Maxwell Construction .....	13
Clausius II Saturation vs NIST Saturation .....	18
Clausius II Representing Metastability .....	19
PvV Validation .....	19
PvT Validation .....	20
CHAPTER IV METASTABILITY RELEVANCE IN ROCKET SYSTEMS .....	21
Catastrophic Occurrences .....	21
Texas A&M Chemistry Lab .....	21
Scaled Compositing Cold Flow (Virgin Galactic) .....	22
Texas A&M 402 .....	23

BLEVE .....	24
Metastability Link To BLEVE .....	25
Conditions of Interest.....	26
<b>CHAPTER V ONE-DIMENSIONAL GAS DYNAMICS .....</b>	<b>28</b>
The 4 Canonical Gas Dynamics Flows .....	28
1D Flow General Form .....	29
Reynolds Transport Theorem .....	29
Mass Conservation .....	30
Conservation of Energy .....	31
Conservation of Momentum According to Kee .....	33
<b>CHAPTER VI CODE SUMMARY .....</b>	<b>34</b>
<b>CHAPTER VII EQUATION OF STATE COMPARISON .....</b>	<b>37</b>
<b>CHAPTER VIII SIMULATION RESULTS .....</b>	<b>39</b>
Fanno .....	39
Results .....	40
Rayleigh.....	41
Results .....	41
Area Variation Based on Kee.....	42
Tank Geometry .....	43
Results .....	44
Combination of Effects .....	46
Rayleigh + Area Variation .....	46
<b>CHAPTER IX MOMENTUM CONSERVATION CORRECTION .....</b>	<b>49</b>
Updated Momentum Conservation Equation .....	49
Updated Chamber Area Results.....	51
Vena Contracta .....	52
Updated Exponential Nozzle Results .....	53
<b>CHAPTER X SUMMARY AND CONCLUSIONS .....</b>	<b>55</b>
Conclusion .....	55
Future Work.....	56
<b>BIBLIOGRAPHY .....</b>	<b>57</b>



## LIST OF FIGURES

FIGURE		Page
1	Cases of Stability .....	4
2	Superheated Transition.....	5
3	Supercooled Transition .....	5
4	Phenomenological picture of metastability in vapor-liquid equilibrium (Modified from [6]) .....	6
5	Impure Phase Transitions vs Metastable Phase Transitions.....	7
6	Vapor Bubble .....	8
7	Maxwell example (Modified from [7]).....	13
8	Maxwell Shift .....	14
9	Maxwell Area .....	16
10	Maxwell Saturation .....	17
11	Maxwell Saturation Comparison .....	18
12	PvV Validation .....	19
13	PvT Validation.....	20
14	Texas AM Chemistry Explosion.....	21
15	Scaled Composites Explosion .....	22
16	Aero 402 Nitrous Oxide Tank Explosion .....	23
17	BLEVE in Nitrous Propellant Tank (Modified from [10]) .....	25
18	Debenedetti Qualitative Metastability (Modified from [6]) .....	26
19	Gas Dynamics .....	28
20	Example Control Volume .....	29

21	Convergence Study.....	35
22	Clausius II vs Ideal Gas.....	37
23	Clausius II vs Ideal Gas.....	38
24	Fanno Results .....	40
25	Rayleigh Results .....	42
26	N2O Tank.....	44
27	Area Variation Results: Pressure v X .....	45
28	Area Variation Results: Pressure v Specific Volume .....	46
29	Rayleigh+Area Variation: Pressure vs x .....	47
30	Rayleigh+Area Variation: Pressure vs Specific Volume .....	48
31	Vena Contracta (Modified from [28]) .....	52

# CHAPTER I

## INTRODUCTION

On July 26, 2007, a liquid nitrous oxide cold flow test resulted in an explosion that killed three and injured three more [11]. The cause of this event was never fully confirmed, with theories relating to chemical reactions being the scapegoat. Events such as this one have been seen multiple times originating from a pressurized tank holding a liquid, some of which will be discussed in chapter 4 of this thesis. The subject of this thesis will be to present research done attempting to identify a more reasonable explanation for these occurrences without the use of chemical reactions.

The chemical reaction explanation for the event is based on work done by Karabeyoglu [27]. His work was able to demonstrate that although nitrous oxide is considered one of the safest oxidizers in liquid and hybrid rocket systems, the rare occurrence of molecular decomposition can result in a large release of thermal energy. Though this theory is sound, what makes it less applicable to the event described is a reliance on either a hot injector or hot gases, which wouldn't be present in a cold flow. Thus, absent external heating of any kind, the only chemical mechanism discussed by Karabeyoglu that may lead to an exothermic reaction would be catalytic decomposition [27]. We postulate a completely different, adiabatic, mechanism which may offer an alternative explanation.

The proposed theory stems from a combination of works, most notably the work done by DeBenedetti on metastable fluids [6] as well as the theorized correlation between BLEVE (Boiling Liquid Expanding Vapor Explosions) and metastable fluids provided by Reid [10]. The work attempts to illustrate a metastable phase change occurring in conditions similar to those which have resulted in explosions, through the use of a 1-Dimensional flow simulation. In order to capture metastable trends through the simulation, a cubic equation of state, Clausius II, was incorporated based on simplifications documented by Emanuel [24].

Metastability itself is the ability of a system to withstand external perturbations up to an energy barrier, beyond which rapid variations of the system occur. When used to describe a phase change,

this describes a system that exists in its original phase beyond the point at which it should have transitioned, but with the existence of any external perturbation, undergoes an explosive transition. Basic equations of state such as the gas law do not capture this effect, instead, more complicated equations of state need to be considered.

By coding a simulation that models a 1-Dimensional flow while accounting for real fluid phase effects, the investigation of a metastable phase transition under realistic flow conditions will be pursued. Including this introduction, the thesis consists of 10 chapters. Following the introduction, chapter 2 will dive deeper into the definitions of metastable phase changes as well as what causes them to occur. Chapter 3 will discuss the decision behind using Clausius II, how it was modeled, as well as a comparison between the thermostatic model and qualitative effects expected in metastable fluids based on DeBenedetti's work. As previously noted, chapter 4 will give an overview of catastrophic events which could be tied to this theory, as well as discuss the relation between metastable fluids and BLEVE theorized by Reid. Chapter 5 will outline the equations used for the 1-Dimensional simulation, while chapter 6 will discuss how the code works. Chapter 7 will demonstrate the variation between results obtained from the gas law equation of state as well as Clausius II, in order to demonstrate the need for its use. Chapter 8 will give preliminary results found, but chapter 9 will discuss a mistake found in Kee's momentum equation derivation [19], offer the correction, and finish with updated results. The conclusion and future work sections will close the thesis in chapter 10.

The work done focused on 1-Dimensional explicit simulations, thus future work will expand on this in order to account for transient effects as well as shocks.

## CHAPTER II

### METASTABILITY AND PHASE CHANGE

#### **Metastability**

When dealing with the stability of a system, there are four cases, under which a system can be identified as stable, which are considered. The first such case is neutral stability, which has the system remaining stable even under perturbations, though the perturbations can cause changes in the system properties. This form of stability is depicted below by showing a ball on a flat plane. If the ball is perturbed in any way, it will easily move to a new position, where it will once again be stable until acted on again. The second case is unconditional stability, which has the system remain stable even under perturbations, but unlike neutrally stable, the system wants to remain at the same initial state. This form of stability is depicted below by showing a ball in a trough. If the ball is perturbed in any way, it will initially move; however, it will want to return to the initial position at which it was stable. The third case is unstable stability, which has the system undergo rapid changes in the presence of perturbations. This form of stability is depicted below by showing a ball on a peak. If the ball is perturbed in any way, it will rapidly roll down the hill and thus not return to a stability condition. The fourth, and most relevant to this work, is metastability. All four cases are depicted in Figure 1.

Metastability allows a system to withstand perturbations up to an energy limit barrier. Once the limit is exceeded, the system is able to undergo rapid and explosive changes. This state of system effects is applicable to fluids undergoing phase transitions. Metastability in fluids is the phenomenon that allows substances to remain at a physical state beyond the point of transition, up to a limit. Substances can be brought to a point where a phase transition is delayed, such as a liquid remaining a saturated liquid past its boiling point, superheating, or a vapor remaining a saturated vapor below its condensation point, supercooling [5]. In order to maintain a metastable state, perturbations, impurities, and surface contact must be limited [9]. The existence of vibrations,

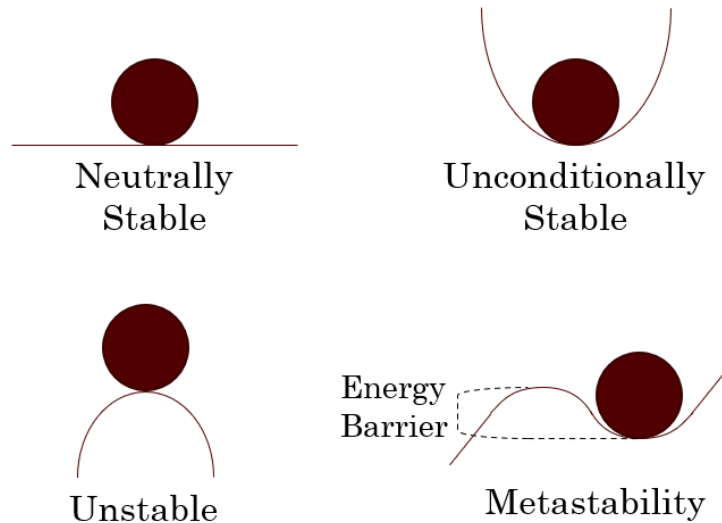


Figure 1: Cases of Stability

suspended impurities, or irregularities on the walls of a container holding a metastable material can lead to a rapid phase transition [6]. This rapid phase transition can occur suddenly and explosively, which is the phenomenon being investigated at present [10][6]. The theory is that housed fluids reach either superheated or supercooled conditions, after which external effects acting on the system result in metastable reactions.

### Phase Change

Occurrences of metastability in phase changes are not simply theoretical, as they can be found experimentally quite simply. The two transition approaches are the perturbation of a superheated liquid, which causes a rapid transition to gas, and the perturbation of a supercooled liquid, which causes a rapid transition to solid. Examples of these two transitions can be found in Figure 2 and Figure 3.

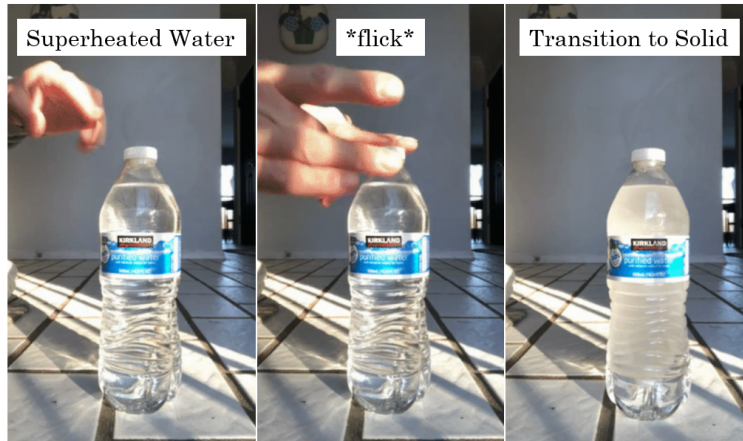


Figure 2: Superheated Transition

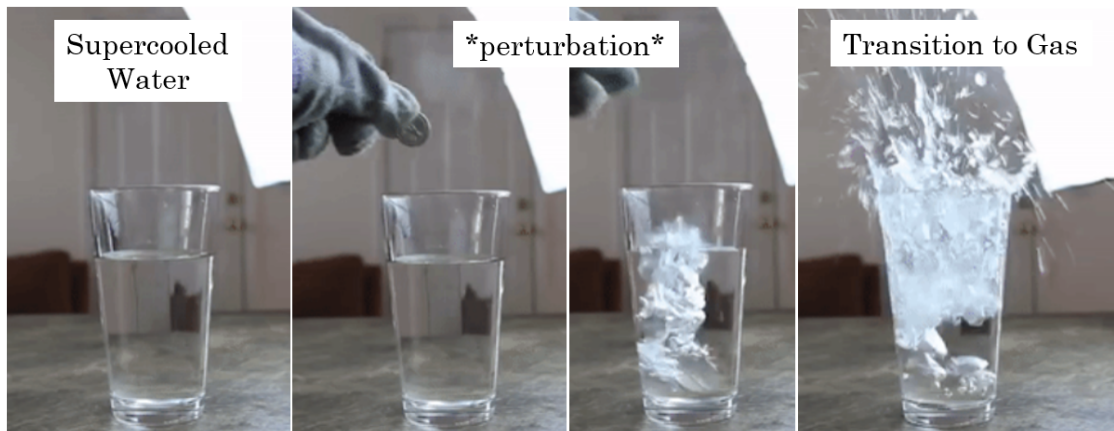


Figure 3: Supercooled Transition

Work done by DeBenedetti helps provide us with qualitative expectations for data representing metastable transitions of fluids [6]. The two main figures of interest for the presented work are the relations between Pressure and Specific Volume as well as the relations between Pressure and Temperature. As can be seen in Figure 4, the Pressure and Specific Volume relation places a cubic isothermal relation passing through the saturation curve. The saturation curve is a curve which separates the phase change from liquid to a vapor. On the left hand side of the saturation curve, the

phase state of the fluid is defined as a liquid. On the right hand side of the saturation curve, the phase state of the fluid is defined as a vapor or gas. The area under the curve houses the range of properties under which the fluid undergoes the phase transition from one state to the other. The peak of the curve is identified as the critical point, of this point, a fluid becomes supercritical, which is an area of interest for research and further work could be done exploring the responses of supercritical fluids in varying flow conditions.

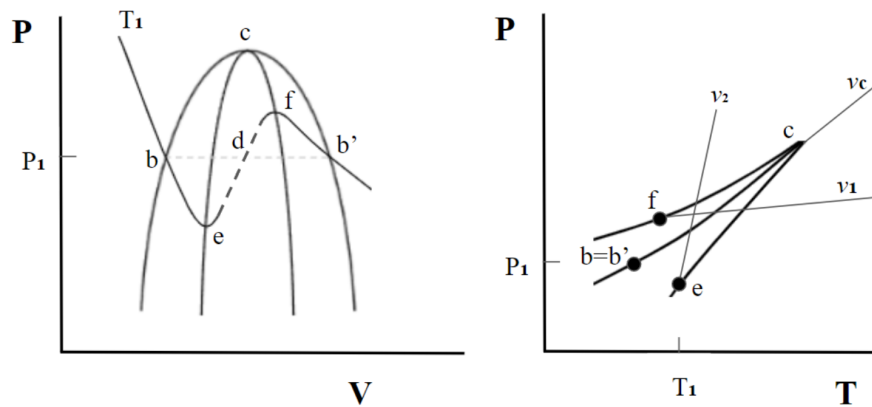


Figure 4: Phenomenological picture of metastability in vapor-liquid equilibrium (Modified from [6])

Figure 4 is a phenomenological picture of metastability in vapor-liquid equilibrium.  $b$  and  $b'$  are equilibrium states on the binodal, where the binodal depicts the saturation bounds.  $e$  and  $f$  are limits of stability on the spinodal, where the spinodal depicts superheating and supercooling. Unstable states are shown by a dashed curve. (b):  $bc b'$  is the binodal and  $ecf$  is the spinodal. (d):  $v_1, v_2, v_c$  are isochores ( $v_1 > v_c > v_2$ ),  $b(= b')c$  is the binodal.  $fc$  is the supercooled vapor spinodal, and  $ec$  is the superheated liquid spinodal [6]. The metastability previously discussed would allow the fluids to reach point  $e$  and point  $f$ . The dashed line between these two points would be the unstable and thus rapid phase transition which we are attempting to model.

Typical phase change models assume a constant pressure through the phase change, in other words passing horizontally from  $b$  to  $b'$ . This approach to phase change modeling is reasonable when



considering a transition which allows phase coexistence between phase states as depicted in the first schematic in Figure 5. These types of transitions are the most common in nature, such as boiling water resulting in steam coexisting with water up until all the water evaporates. The method of constant pressure treats common impure fluids through a stable phase change, but as such doesn't produce the explosive phase changes in metastable fluids which are of interest. Instead, a separate phase transition model approach must be taken.

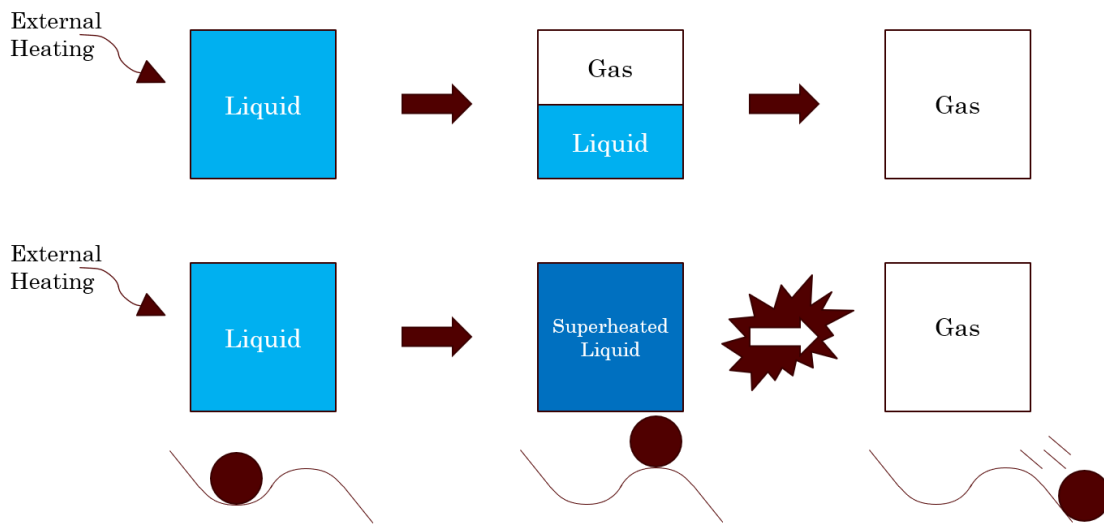


Figure 5: Impure Phase Transitions vs Metastable Phase Transitions

The first step taken was deciding on how to thermostatically model metastable behavior. This will be tackled in the following chapter.

### Superheated Liquid

Since the main topic of investigation will be superheated liquids, a more in-depth explanation of the phenomenon will be given. A liquid is considered superheated once the temperature at which it exists is higher than the boiling point, while also having its phase remain unchanged.

The physical cause of superheating originates from surface tension. Surface tension is a property of a liquid that allows it to resist external forces as a result of the cohesion between its molecules

[33]. A phase transition from liquid to gas can be visualized by the formation of bubbles in the liquid, this demonstrates a body of vapor housed in a liquid, but separated by the surface tension around the vapor [32].

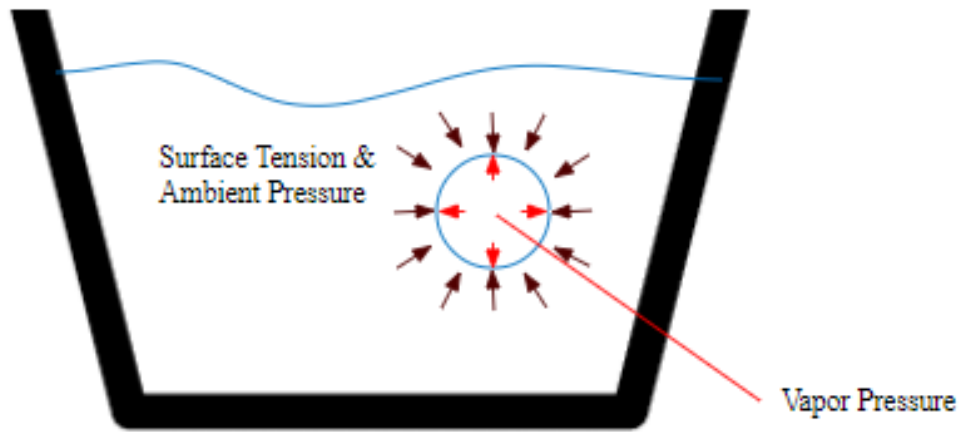


Figure 6: Vapor Bubble

Under the existence of imperfections or stimuli, large bubbles will form, further stimulating the system which causes the typical phase change. The existence of larger bubbles also reduces the pressure differential or stimuli required to overcome surface tension. If instead of the formation of large bubbles, only small and stable bubbles form, the pressure differential required to overcome the surface tension becomes much bigger [32]. Under an unperturbed condition, the system thus is able to remain liquid beyond the boiling point [32]. Once an external stimuli is added to the system, a rapid chain begins rupturing all the small bubbles and causing the perceived explosive rapid phase change.

## CHAPTER III

### MODELING METASTABILITY

#### **Equations of State**

Equations of states are models which attempt to produce relations between fluid properties such as pressure, volume, and temperature. In order to effectively do so, most equations of state make assumptions and simplification which allow them to be valid for a specific range of conditions. The most common equation of state that can be seen in practice is the Ideal Gas Law ( $PV = nRT$ ), but this is only valid for perfect gases. In many cases when considering gases, the assumption of thermally and calorically perfect gas is valid and simplifies the analysis; however, this approach is only valid for conditions away from phase change and the critical point, and prior to when high temperatures cause vibrational effects to play a larger effect. In place of the thermal state equation for a perfect gas, many thermal state equations have been developed which focus on other ranges of fluid properties [2].

Based on the metastable relations shown by Debenedetti [6], and depicted in Figure 4, the relation between Pressure and Volume follows a trend that is, at minimal, cubic in nature. In the spirit of simplicity, a cubic equation of state was selected to qualitatively model metastable behaviour. For the topic of this paper, the application and comparison to measured data will be looked into for Clausius II.

#### **Clausius II Equation of State**

The formulation for the thermodynamic equations used in this paper starts from the thermal state equation under Clausius II [2].

The derivation will begin with the base version of Clausius II.

$$p = \frac{RT}{c - b} - \frac{a}{T(v + c)^2} \quad (1)$$

$$a = \frac{27 RT_c v_c}{64 Z_c}$$

$$b = v_c \left(1 - \frac{1}{4z_c}\right)$$

$$c = v_c \left(-1 + \frac{3}{8} \frac{1}{Z_c}\right)$$

Equation 1 is one of the many possible thermal EOS which can be used to describe deviations of real gases/dense vapors from the perfect (ideal) gas model and its EOS ( $pv = RT$ ).<sup>1</sup> One of these constants ( $b$ ) is more fundamental than the others, since it relates to the “co-volume” of the species, i.e. it relates to the size of the molecule and how that size creates dense-vapor effects when the molecules are brought together at high densities. Subscript “ $c$ ” denotes the critical point of the species in question:  $Z_c$  is the compressibility factor at the critical point, which is found from  $Z_c = P_c V_c / RT_c$ , and can be used to describe the deviation of a real gas at the critical state from the ideal gas model, since  $Z_c = 1$  for ideal gases, while  $Z_c \approx 0.23$  for many species.

The Clausius II model needs to be augmented with the caloric EOS describing internal energy, as well as equations describing entropy behavior, chemical potential, and all possible higher order thermodynamic coefficients resulting from Maxwell relations. These result from laborious, if straightforward manipulations that can be found in advanced Thermodynamics textbooks (e.g. [2, pp. 151-158]). Here only the major, salient results used in the calculation are shown.

Equation 1 is transformed into its reduced variable form in order to simplify the equations that will be solved.

$$A = 1 + 4Z_c(v_r - 1)$$

$$B = 1 + \frac{8}{3}Z_c(v_r - 1)$$

---

<sup>1</sup>The Clausius II model is using three constants ( $a, b, c$ ) to describe dense-vapor effects, while one of the most well-known models, and the first one to be formulated is the van der Waals model

$$p = \frac{RT}{v - b} - \frac{a}{v^2}$$

which uses two constants to describe real-gas effects.

The two constants  $A$  and  $B$  are introduced here for convenience. The thermodynamic equations are used in their respective reduced variable forms, i.e.

$$p_r = \frac{p}{p_c}, T_r = \frac{T}{T_c}, v_r = \frac{v}{v_c}$$

The reduced variable form of Clausius II thermodynamics equations used in the code documented in this paper are as follow:

$$p_r = \frac{4T_r}{A} - \frac{3}{T_r B^2} \quad (2)$$

$$s_r = 1 + \frac{9R}{8s_c} \left(1 - \frac{1}{T_r^2 B}\right) + \frac{R}{s_c} \ln(A) + \frac{1}{s_c} \int_1^{T_r} c_v^o(T'_r) \frac{dT'_r}{T'_r} \quad (3)$$

$$u_r = 1 + \frac{9RT_c}{4u_c} \left(1 - \frac{1}{T_r B}\right) + \frac{T_c}{u_c} \int_1^{T_r} c_v^o(T'_r) dT'_r \quad (4)$$

$$\begin{aligned} \frac{\mu}{RT_c} = \frac{u_c - T_c s_c}{RT_c} + \frac{9}{8} \left(2 - T_r - \frac{1}{T_r B^2} \left(1 + \frac{8}{3} Z_c (2v_r - 1)\right)\right) + 4Z_c \frac{v_r T_r}{A} \\ - T_r \ln(A) + \frac{1}{R} \int_1^{T_r} c_v^o(T'_r) \left(1 - \frac{T_r}{T'_r}\right) dT'_r \end{aligned} \quad (5)$$

In the above set of equations (2-5) describing the Clausius II model almost all properties and parameters can be calculated explicitly; the ideal-gas specific heat ( $c_v^o$ ) may be evaluated as a function of temperature, or even be considered a constant during the calculations.

It is important to note that, like many of the equivalent real-gas/dense vapor EOS, the Clausius II model is valid only in certain areas of the thermodynamic phase diagram, notably near the critical point, where the values for many of the associated constants are evaluated, as well as near the perfect gas limit, where the ideal EOS must be recovered. The goal of the present work is to use one of the simplest “cubic” equations of state to show– qualitatively–metastable behavior, and to

examine the possibility of BLEVE in liquid-propellant rocket systems. As the work concentrates more on the liquid phase of the nitrous propellant, and attempts to show transition from the liquid to the vapor spinodal, the behavior of the model is expected to be strictly qualitative, particularly for conditions far from the critical.

### **Clausius II Liquid-Vapor Coexistence**

Because of the qualitative character of the thermal and caloric EOS under use, the actual liquid-vapor coexistence (saturation) curve derived by experiments, and tabulated in databases such as NIST are not taken as consistent with the model [26]. To be internally consistent in this work, the properties of the saturation line need to be derived from the Clausius II model itself.

In order to obtain a plot for saturation data based on the Clausius II formulation, Maxwell Construction was implemented into the code. This step was taken in order to compare with NIST data as a form of accepting the data output from the model as reasonably realistic.

#### *Maxwell Construction*

Proposed by James Clerk Maxwell, Maxwell Construction is an approach to thermal state equations which uses the saturation curve in order to derive the spinodal curves; however, the inverse will be done here, using the spinodal curves in order to find saturation points. The direct quote from James Clerk Maxwell: “Now let us suppose the medium to pass from B to F along the hypothetical curve BCDEF in a state always homogeneous, and to return along the straight line path FB in the form of a mixture of liquid and vapour. Since the temperature has been constant throughout, no heat can have been transformed into work. Now the heat transformed into work is represented by the excess of the area FDE over BCD. hence the condition which determine the maximum pressure of the vapour at given temperature is that the line BF cuts off equal areas from the curve above and below.” [7]

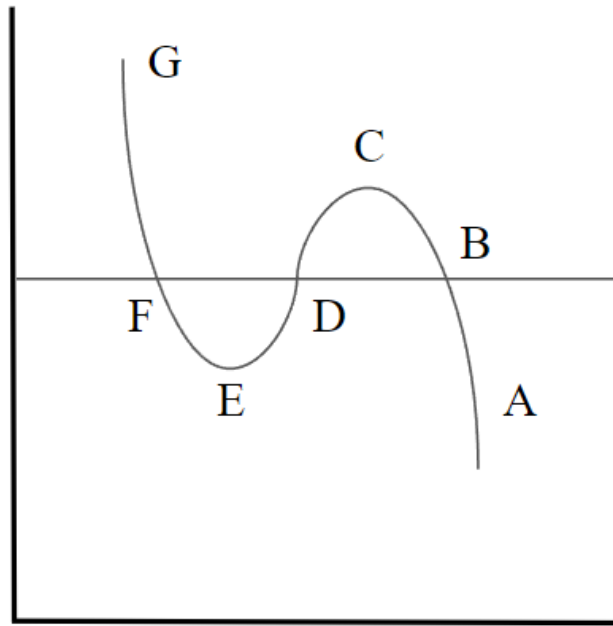


Figure 7: Maxwell example  
(Modified from [7])

### *Application of Maxwell Construction*

In order to apply Maxwell Construction, the following steps were followed:

- "Draw" a horizontal line through the isotherm.
- Solve for the two areas created by the horizontal line and the isotherm.
- Compare the areas and shift the horizontal line until the areas are equal.
- Save the outer  $V_r$  points as they will make up the stagnation diagram.

In order to get this to work, the first step taken was to create a function for  $P_r$  assuming a constant  $T_r$ . The  $T_r$  value would be varied, as such creating a range of isotherms on a  $P_r$  vs  $V_r$  plot. Starting from the first isotherm, the drawing of the horizontal line is accomplished by shifting the plot down

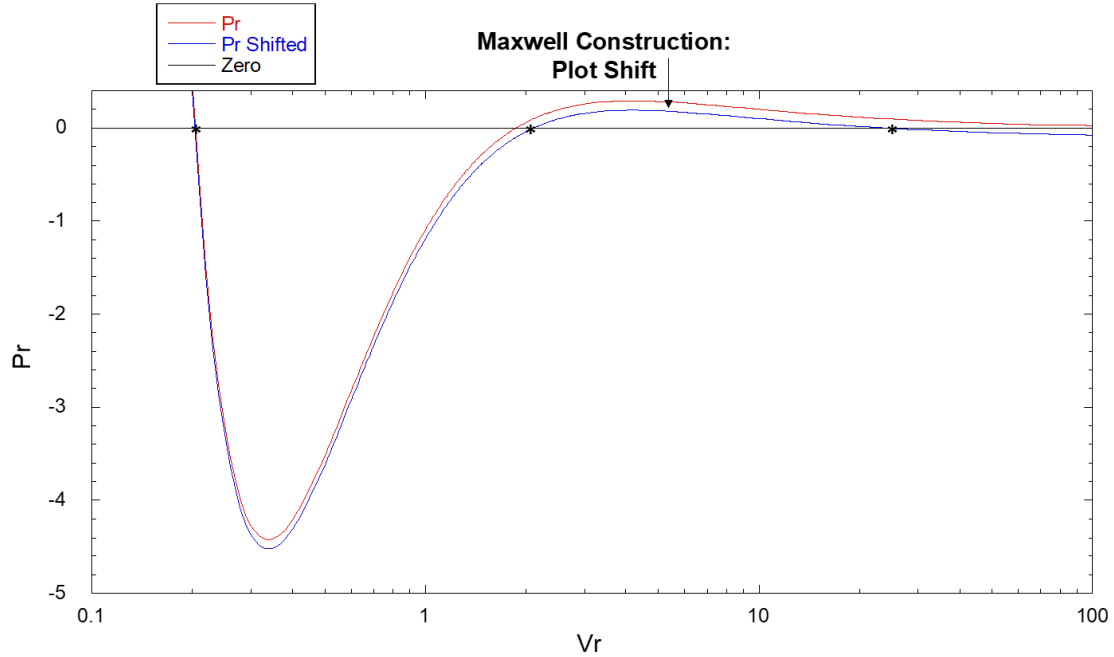


Figure 8: Maxwell Shift

such that the peak intersects a  $P_r = 0$ . From there, the function would be shifted up creating three intersect points through zero, as shown in Figure 8.

Newton's method was used on the shifted function in order to find the three roots of the function, these are denoted by "\*" in Figure 8. The definite integral was calculated between the first two roots as Area 1 and between the second two roots as Area 2.

Starting from the  $P_r$  function, the definite integral was evaluated between the points:

$$A = 1 + 4Z_c(v_r - 1)$$

$$B = 1 + \frac{8}{3}Z_c(v_r - 1)$$

$$p_r = \frac{4T_r}{A} - \frac{3}{T_r B^2} - \text{Shift}$$



$$p_r = \frac{4T_r}{1 + 4Z_c(v_r - 1)} - \frac{3}{T_r(1 + \frac{8}{3}Z_c(v_r - 1))^2} - \text{Shift}$$

$$\int p_r dv_r = \frac{27}{8T_r Z_c(8Z_c(v_r - 1) + 3)} + \frac{T_r \ln |4Z_c(v_r - 1) + 1|}{Z_c} + \text{Shift} * v_r$$

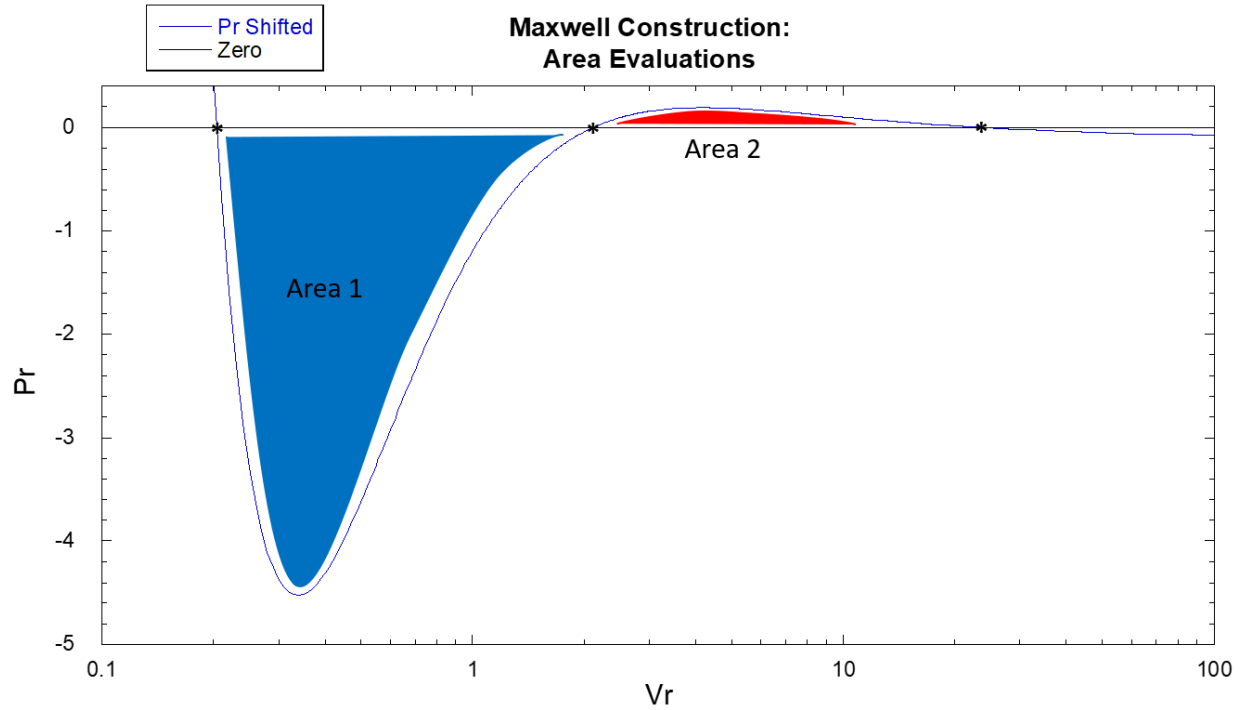


Figure 9: Maxwell Area

Based on a preset tolerance, the absolute value of the definite integrals (i.e. the two areas), were compared. If the difference in values was less than the tolerance, the first and third root were recorded as they, by definition, lie on the saturation curve.

If the areas do not fall within the tolerance, the isotherm was shifted more. This repeats until the areas do fall within the tolerance. These steps are repeated for a range of isotherms in order to adequately fill out a saturation plot.

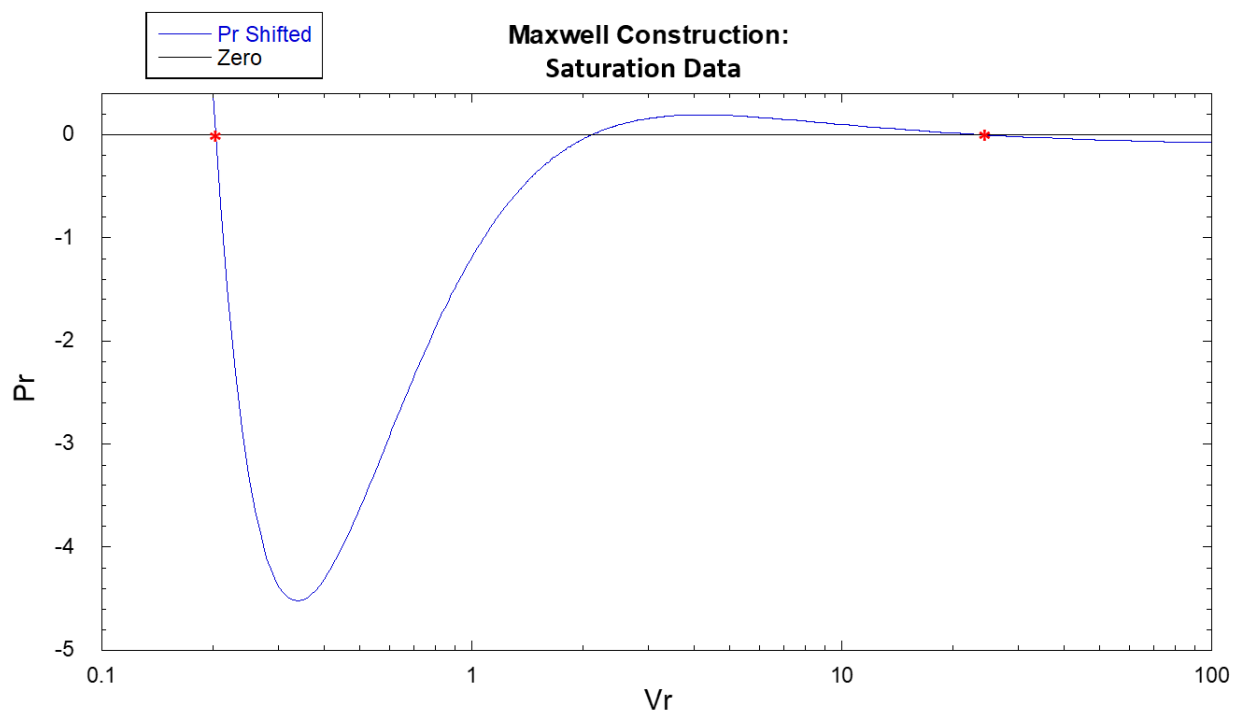


Figure 10: Maxwell Saturation

## Clausius II Saturation vs NIST Saturation

Experimental results have been obtained from NIST for  $N_2O$  [26]. Below, the comparison between NIST and Clausius II is shown. Good agreement, with slight variance as is expected from a model, is obtained. This allows us to have a saturation plot based on on Clausius II to overlay on future simulations, specifically tied to the Clausius II equation instead of experimental data.

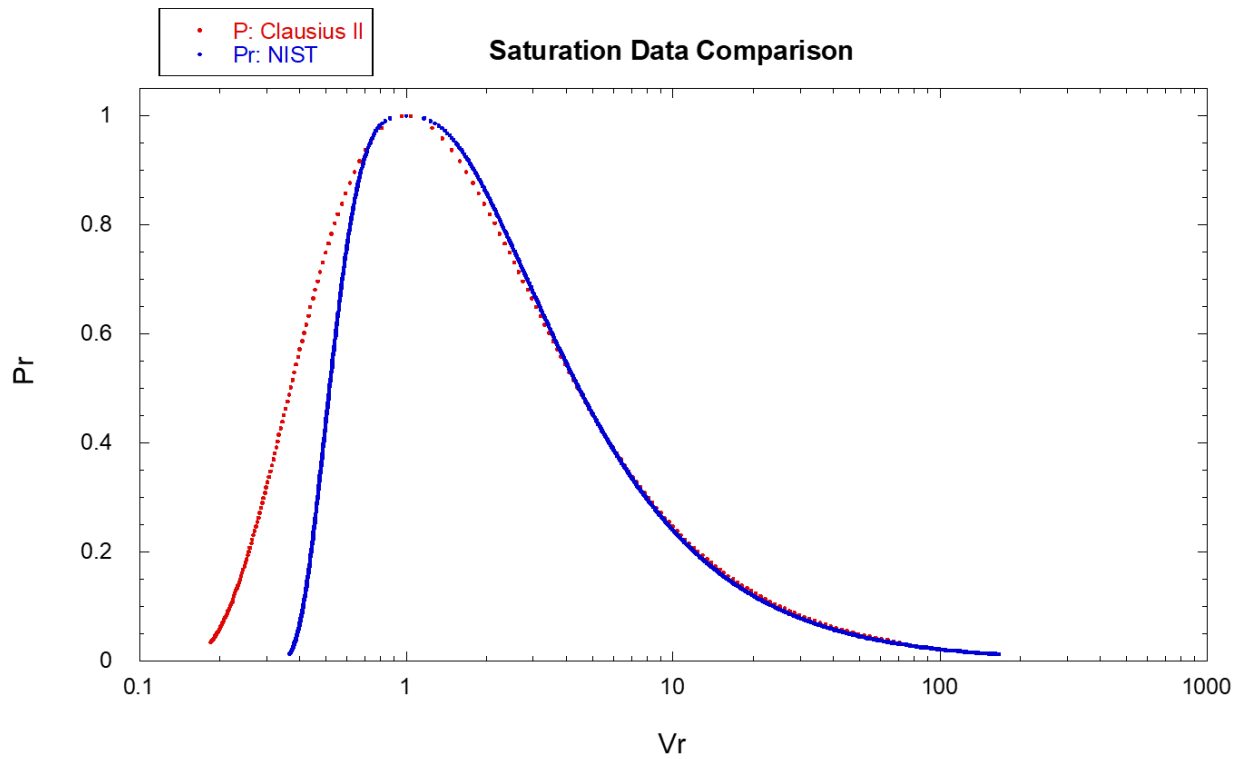


Figure 11: Maxwell Saturation Comparison

## Clausius II Representing Metastability

### PvV Validation

The Maxwell Construction combined with Clausius II was used in our model in order to reproduce metastability trends. Negative pressure trends shown below are attributed to surface tension effects, though the goal is to stay away from this area of the plot as accuracy decreases as distance from the critical point increases. Comparing the qualitative plot produced by DeBenedetti, as reproduced in Figure 12a, with the plot generated by the developed Clausius II code, as shown in Figure 13b, the trends align, thus allowing the developed code to be valid for use in reproducing metastable trends [6].

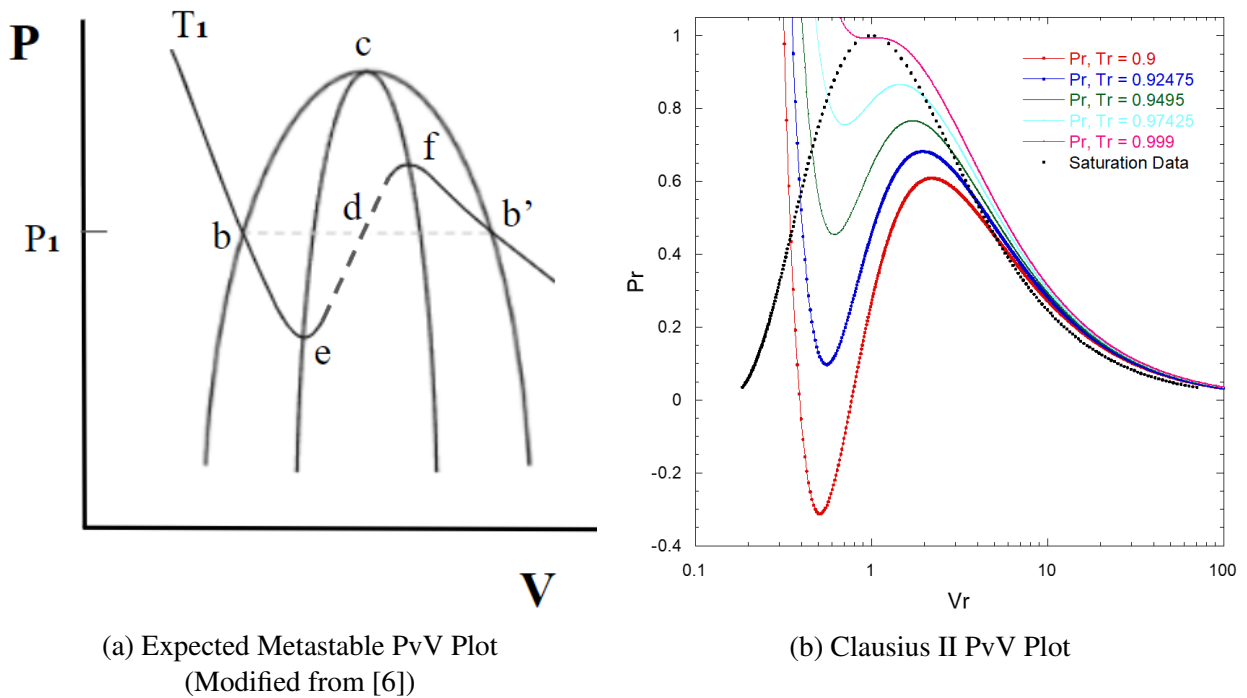


Figure 12: PvV Validation

## PvT Validation

Clausius II supercooled and superheated spinodals were used in order to reproduce similar trends as those expected based on the Debenedetti work [6].

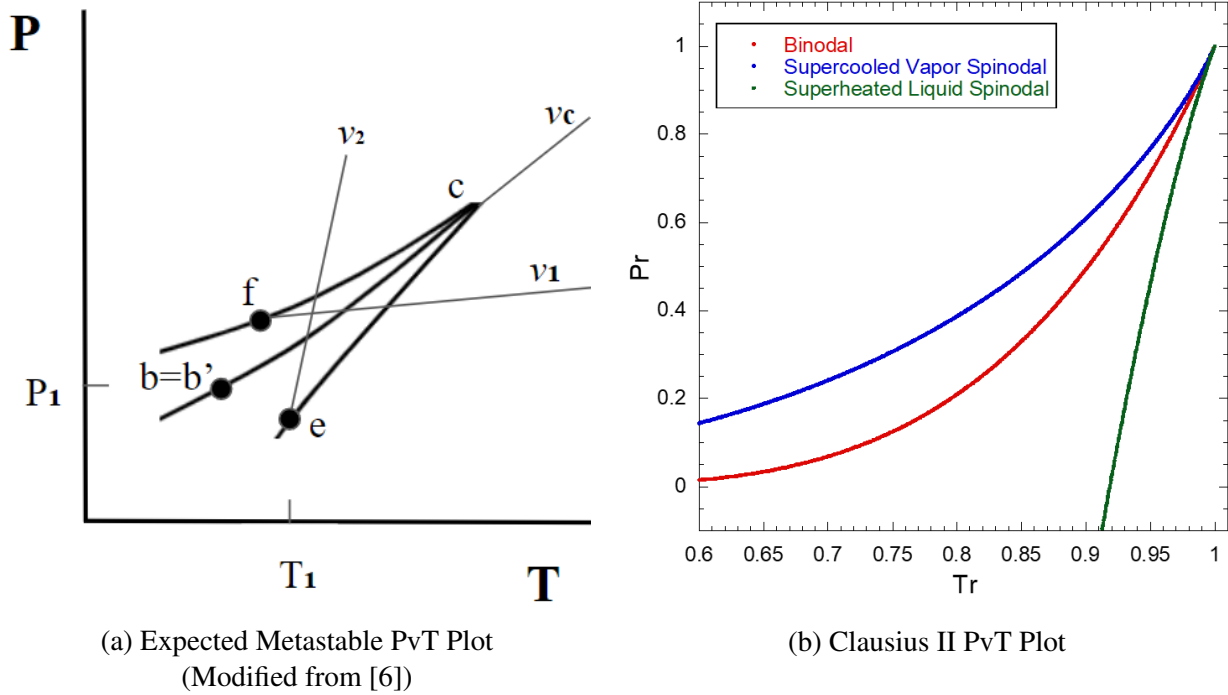


Figure 13: PvT Validation

## CHAPTER IV

### METASTABILITY RELEVANCE IN ROCKET SYSTEMS

#### Catastrophic Occurrences

##### Texas A&M Chemistry Lab

On January 12, 2006, a liquid nitrogen tank whose internal pressure relief devices had been removed and openings sealed, exploded. The explosion of the tank resulted in severe damage to the lab housing it as shown in Figure 14 [23]. Although no one was injured by this event, it was still catastrophic.



Figure 14: Texas AM Chemistry Explosion

From the State Marshal's Alert, "The resulting examination revealed catastrophic failure of the cylinder. The failure permitted rapid expansion of the nitrogen gas, blowing out the bottom of the tank and propelling the cylinder upwards"[23]. The rapid phase change from liquid in the

container to gas exiting the container is reminiscent of the metastable phase changes depicted in Chapter 2. The incident gives a benchmark of the geometric and system conditions which may cause a possible metastable phase change, a rapid escape of liquid through a small crack. This example seems to highlight area variation as a component of interest for the investigation being conducted.

### **Scaled Composites Cold Flow (Virgin Galactic)**

On July 26, 2007, a liquid nitrous oxide cold flow exploded causing the death of three engineers and injuring three others at Scaled Composites in Mojave, California [11].

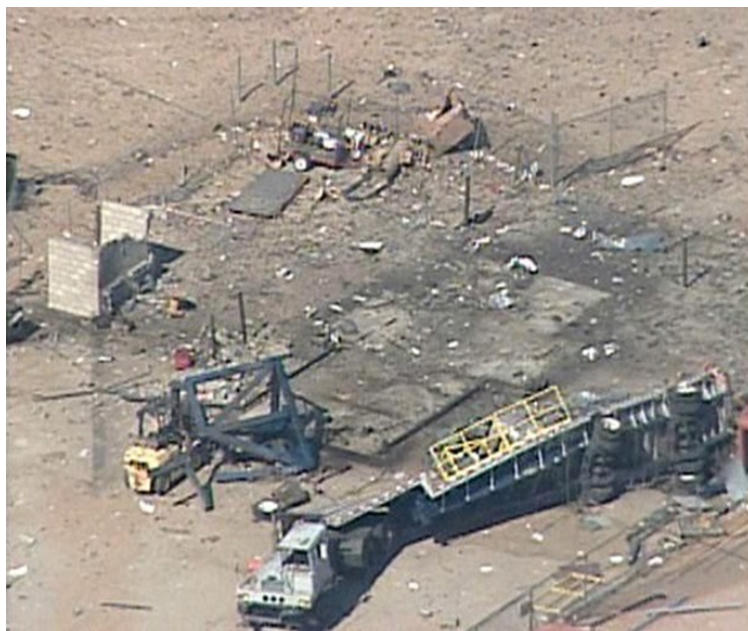


Figure 15: Scaled Composites Explosion

A cold flow is a test used to check that fluids travel through engines correctly and are correctly distributed. As such, there is no ignition of the fluid used, liquid nitrous oxide. This is why it was a terrifying surprise when 3 seconds into the test, the tank of liquid nitrous oxide exploded. The actual cause of the event was left a mystery. Scaled Composites founder Burt Rutan's response



when asked on what caused the accident, "We just don't know" [11]. An investigation conducted by OSHA was still unable to determine a cause, the only insight given was that previous research had shown that nitrous oxide could explode if it came into contact with easily oxidized materials [11] [27]. The chemical reaction explanation being a cause of the explosion isn't certain, thus the possibility of a metastable phase change being at the route of the explosion remains a possibility. The aim of the current work is to attempt to show the possibility of such a link, while negating any chemical effects. It was also noted that the day was labeled as "hot", which raises an interest in external heating possibly aiding in a metastable phase transition.

### **Texas A&M 402**

The third example which will be discussed also occurred at Texas A&M. A cold flow was being run for an AERO 402 class, but the nitrous oxide tank unexpectedly exploded. A piece of the tank was recovered and is pictured in Figure 16.



Figure 16: Aero 402 Nitrous Oxide Tank Explosion

Though no direct cause was found, initial speculation was based around the Scaled Composites case, once again noting the research on nitrous oxide reactivity. No further investigation was conducted, leaving the door open for other explanations. The benefit of this event, was that with a portion of the tank recovered, a geometry now was available to incorporate in the model which had had an explosion in the conditions which we believed metastable phase changes could occur.

## **BLEVE**

Up to this point, the description of a metastable phase change has been used; however, many more occurrences related to tank explosions have happened. These types of explosions have been dubbed BLEVE (Boiling Liquid Expanding Vapor Explosions).

The following are excerpts from the National Fire Protection Association's *Guide to Fire and Explosion Investigations*.

“While the initiating event can be caused by a vessel failure (fire or mechanical fault), the explosion and overpressure associated with a BLEVE is due to expansion of pressurized gas or vapor in the ullage (vapor space) combined with the rapidly boiling liquid liberating vapor” [1].

“A BLEVE may also result from a reduction in the strength of a container as a result of mechanical damage or localized heating above the liquid level. This rupture of the confining vessel subjects the pressurized liquid to a sudden drop in pressure and allows it to vaporize almost instantaneously, contributing to the overpressure and explosion” [1].

The descriptions provided closely correlate to the examples previously discussed, as well as the conditions of metastable phase changes. In order to correlate the two events, the presented works acts as an attempt to demonstrate a metastable phase change through the use of conditions present in the cases of BLEVE most likely linked to metastability.

## Metastability Link To BLEVE

The theory for a possible metastable phase change link to BLEVE has been previously approached by Reid [10]. The work focused on adiabatic conditions, which are valid when considering a cold-flow as external heating is mostly negligible. The figure shown below was a reproduction of a Reid figure using the Clausius II model developed.

The figure on the left depicts a propellant run tank, connected to the solid motor through piping and valves. The plot below on the right depicts two different cases for the fluid in the run tank to transition from its initial saturated liquid state (*a* or *b*) to a different final state (liquid or vapor respectively) [10].

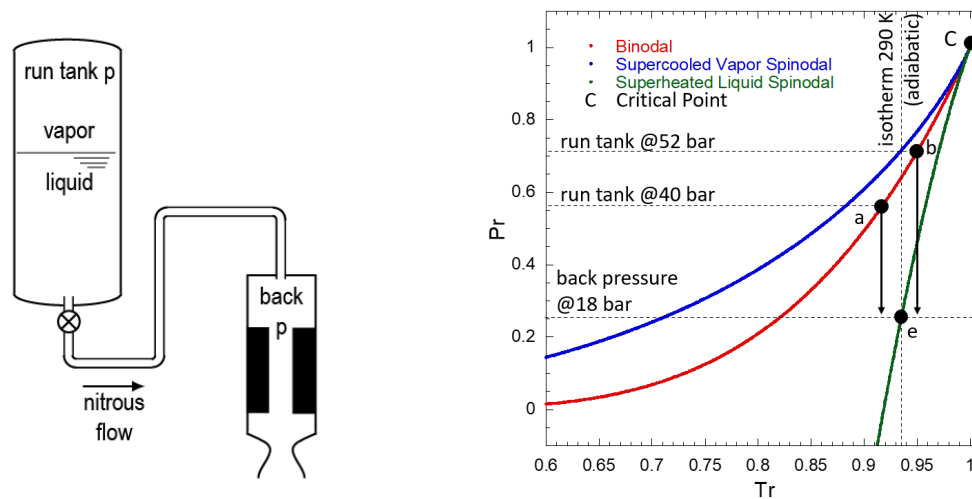


Figure 17: BLEVE in Nitrous Propellant Tank  
(Modified from [10])

In the essence of theorizing a case of BLEVE without heating, an adiabatic trend is illustrated. Two possible cases are depicted above: (a) at 40 bar and 285 K or (b) at 50 bar and 296 K. Either one of these cases are possible when using a nitrous oxidizer in a blow-down. With an assumption of 18 bar of back pressure present at the exit (e), which is a realistic value for a rocket chamber pressure, paths for the phase conditions are theorized. During the adiabatic pressure drop depicted by the

arrows, two cases are shown: (a) reaches the back pressure without crossing the liquid spinodal; however, (b) does cross the superheat limit and thus results in the previously discussed explosively rapid transition to vapor. This is best illustrated by looking at Debenedetti's qualitative metastability diagram, depicted once again in Figure 18.

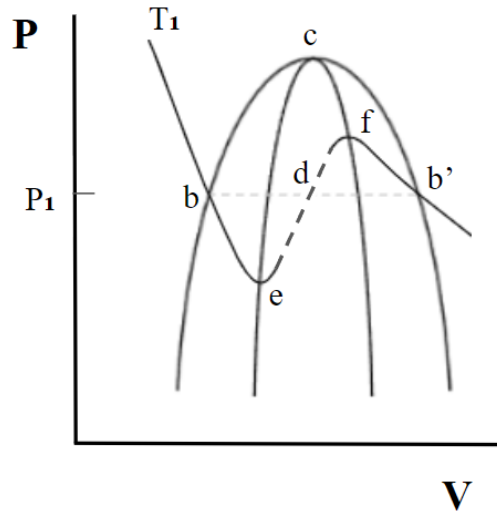


Figure 18: Debenedetti Qualitative Metastability  
(Modified from [6])

What occurs, is that the initial condition has the fluid at properties  $b$ . The final properties would require a pressure value below  $e$ , thus is can't be reached unless it goes to  $e$ , then quickly transitions to  $f$ , from which it is free to drop to the pressure required by the final properties. Case (b) would be a possible theoretic demonstration of adiabatic BLEVE occurring [5] [10].

### Conditions of Interest

There are two conditions tied to BLEVE which the presented work hoped to give a better understanding of.

The first condition involves the continued heating of a pressurized tank through events such as a fire or extreme levels of sunlight, which will result in an increase of internal pressure. Once the

internal pressure exceeds that which the tank can safely hold, initial cracking of the tank will begin to develop. The simulations run analyze specifically this moment. As the high velocity liquid escapes through the crack, an instantaneous phase conversion can occur, thus leading to rapid fluid expansion. Coupling the expansion with the high pressure, the holding tank would be ripped apart resulting in the explosion seen in cases of BLEVE.

The second condition involves the rapid release of a fluid through a channel with significant area variation, while coupled with external heating and/or internal friction. The idea behind this analysis, is that choking of the fluid could be induced by the channel dimensions, but heating and/or friction could result in this occurring sooner and thus leaving an area with the potential of rapid phase changes occurring. Once more, the idea is that this rapid phase change would result in an explosion as seen in cases of BLEVE.

CHAPTER V  
ONE-DIMENSIONAL GAS DYNAMICS

**The 4 Canonical Gas Dynamics Flows**

When considering gas dynamics, though in the presented case the fluid will begin as a liquid, there exist dynamic flows which are attributed to property changes. The three such dynamic flows which were analyzed are depicted in Figure 19. These are investigated in the hope that they can cause fluid property changes demonstrating metastable phase changes.

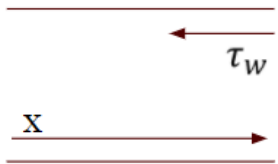

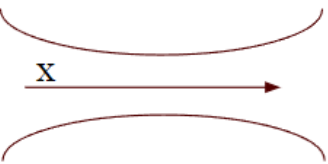
1) Fanno (friction)	2) Rayleigh (heat)	3) Area Variation
		
$dA = 0$ $\delta f \neq 0$ $\delta q = 0$ $ds \neq 0$	$dA = 0$ $\delta f = 0$ $\delta q \neq 0$ $ds \neq 0$	$dA \neq 0$ $\delta f = 0$ $\delta q = 0$ $ds = 0$

Figure 19: Gas Dynamics

Fanno is the consideration of wall shear as a results of the fluid's interaction with the wall from friction. This uses a friction factor which is based on the channel geometry, fluid properties, wall roughness, and flow speed. Pure Fanno flow has no heating or area variation considered.

Rayleigh is the consideration of external heating to the system from factors such as sunlight or fires. The heating term here is arbitrary since it fully depends on external conditions. Pure Rayleigh flow has no friction effects or area variation considered.

Area variation is the consideration of a channel with changing geometry along  $x$ . The area variation employed will be based around the recovered tank from the Texas A&M 402 Nitrous Oxide explosion. Pure area variation has no heating or friction considered.

After investigation of the effects individually, the combined effects will also be investigated.

### 1D Flow General Form

Derivations following [19] were utilized, based around a control volume as depicted in Figure 20, in order to develop a one-dimensional flow simulation.

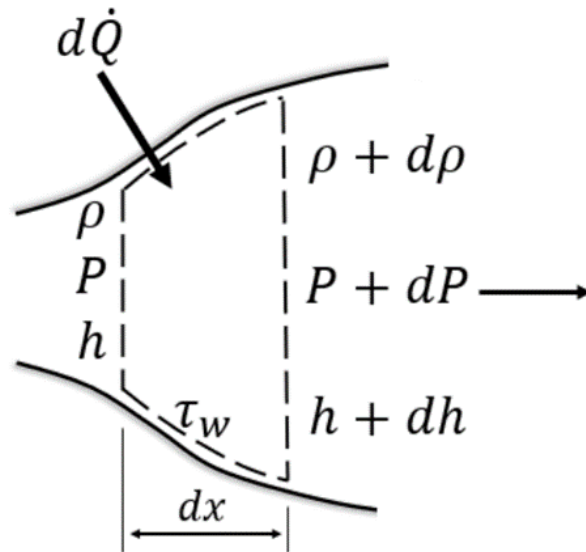


Figure 20: Example Control Volume

### Reynolds Transport Theorem

Reynolds transport theorem will be applied multiple times in the derivations of the conservation equations, thus an overview of it will be given.

When considering a system for which properties will be analyzed, there are two manners of approaching the system. The first is system approach is that of a closed system. A closed system is a

system which doesn't allow mass to cross its boundaries; however, energy, such as that provided by heat or work, is free to cross [30]. The second system approach is that of an open system. An open system is a system which allows both energy and mass to pass through its boundaries. These two systems, typically referred to as *Lagrangian* for closed and *Eulerian* for open for the mathematicians which coined each technique, though different in approach, must arrive at the same result [30]. Since this must be the case, a mathematical approach must exist which is able to transform the conservation equation between the two frames, this approach is the Reynolds transport theorem [30].

Though the full derivation of the Reynolds transport theorem will not be presented here, fluid mechanics textbooks can be consulted for this. The main points begin by defining the rate of gain of property  $X$  by a closed, Lagrangian, system through the term  $\frac{DX}{Dt}$ . This term denotes that the mass remains fixed in the system. The Reynolds transport theorem allows the following relation to be applied [30]:

$$\frac{DX}{Dt} = \int_V \frac{\partial(\rho x)}{\partial t} dV + \int_A \rho x (\mathbf{V} \cdot d\mathbf{A})$$

The term on the left depicts the closed system rate, while the system on the right depicts the open system rate. There is also a property difference between the two,  $x = \frac{X}{m}$ , such that  $x$  is the specific version of  $X$ .

### **Mass Conservation**

Starting with the mass conservation of the system negating chemical reactions, since we aim to provide a non-chemically-related explosion:

$$\left(\frac{dm}{dt}\right)_{sys} = 0$$

Assuming steady flow and applying Reynolds transport theorem, the equation becomes:



$$\int_{CS} \rho \mathbf{V} \cdot \mathbf{n} dA = 0$$

The integral is then evaluated directly on each portion of the control surface. Recalling that the orientation of the surfaces is described by the outward-normal unit vector  $\mathbf{n}$ , the mass-conservation equation becomes:

$$-\rho u A_c + \left( \rho u A_c + \frac{d(\rho u A_c)}{dx} \right) dx = 0$$

Simplifying this equation, the final equation for mass conservation which will be used in the following derivations is [19]:

$$\boxed{\frac{d(\rho u A_c)}{dx} = 0}$$

### Conservation of Energy

Continuing forth, the energy conservation of the system starts as:

$$\frac{dE}{dt} = \frac{dQ}{dt} + \frac{dW}{dt}$$

Using the Reynolds transport theorem with internal energy,  $e$ , as the intensive variable, while negating potential energy effects, results in:

$$\int_{CS} \rho \left( e + \frac{u^2}{2} \right) \mathbf{V} \cdot \mathbf{n} dA = d\dot{Q} - \int_{CS} \rho \mathbf{V} \cdot \mathbf{n} dA$$

Moving the integral on the right into the integral on the left allows us to simplify the equation:

$$\int_{CS} \left( e + \frac{P}{\rho} + \frac{u^2}{2} \right) \rho \mathbf{V} \cdot \mathbf{n} dA = d\dot{Q}$$

Using the definition of enthalpy,  $h = e + P/\rho$ , and following the assumption of no velocity term aside from velocity along  $x$ , and evaluating the integral, the equation becomes:

$$\int_{CS} \nabla \cdot \rho h \mathbf{V} dV + \int_{CS} \nabla \cdot \rho \left( \frac{u^2}{2} \right) \mathbf{V} dV = d\dot{Q}$$

$$\frac{d(\rho u h A_c)}{dx} + \frac{d(\rho u \frac{u^2}{2} A_c)}{dx} = \frac{d\dot{Q}}{dx}$$

Expanding the differential terms will allow us to remove extra terms:

$$\rho u A_c \frac{dh}{dx} + h \frac{d(\rho u A_c)}{dx} + \rho u A_c \frac{d\left(\frac{u^2}{2}\right)}{dx} + \frac{u^2}{2} \frac{d(\rho u A_c)}{dx} = \frac{d\dot{Q}}{dx}$$

Recalling the result from mass conservation  $\frac{d(\rho u A_c)}{dx} = 0$ :

$$\rho u A_c \frac{dh}{dx} + \rho u A_c \frac{d\left(\frac{u^2}{2}\right)}{dx} = \frac{d\dot{Q}}{dx}$$

$$\rho u A_c \frac{dh}{dx} + \rho u A_c \frac{u du}{dx} = \frac{d\dot{Q}}{dx}$$

Setting  $\dot{m} = \rho u A_c$  [19]:

$$\dot{m} \frac{dh}{dx} + \dot{m} \frac{u du}{dx} = \frac{d\dot{Q}}{dx}$$

$$\frac{dh}{dx} + \frac{u du}{dx} = \frac{1}{\dot{m}} \frac{d\dot{Q}}{dx}$$

$$\boxed{\frac{dh}{dx} + \frac{u du}{dx} = \frac{dq}{dx}}$$

## Conservation of Momentum According to Kee

The velocity and pressure profiles throughout the channel are related through the momentum equation.

$$\int_{CS} \rho \mathbf{V} \cdot \mathbf{V} \cdot \mathbf{n} dA = - \int_{CS} P dA - \int_{CS} \tau_w dA$$

Assuming a variable-area channel and a steady-state flow, the integrals can be evaluated for the differential control volume as [19]:

$$-\rho u^2 A_c + \left( \rho u^2 A_c + \frac{d(\rho u^2 A_c)}{dx} dx \right) = P A_c - \left( P A_c + \frac{d(P A_c)}{dx} dx \right) - \tau_w C dx$$

Where  $C$  is the circumference of the channel and  $\tau_w$  is the shear force from wall friction. Cancelling like terms leaves the following equation:

$$\frac{d(\rho u^2 A_c)}{dx} dx = \frac{d(P A_c)}{dx} dx - \tau_w C dx$$

$$\frac{d(\rho u^2 A_c)}{dx} = \frac{d(P A_c)}{dx} - \tau_w C$$

Expanding the derivative:

$$\rho u A_c \frac{du}{dx} + u \frac{d(\rho u A_c)}{dx} = - \frac{d(P A_c)}{dx} - \tau_w C$$

Recalling the result from mass conservation  $\frac{d(\rho u A_c)}{dx} = 0$  and expanding the remaining derivative further gives the final equation of momentum conservation which will be used [19]:

$$\boxed{\rho u A_c \frac{du}{dx} = -P \frac{dA_c}{dx} - A_c \frac{dP}{dx} - \tau_w C}$$

CHAPTER VI  
CODE SUMMARY

1. Initial conditions are set: Pressure, Temperature, Velocity, Acceleration, Friction, Heating, and channel dimensions.
2. Clausius II code is utilized in combination with initial conditions to give all other initial fluid properties that will be needed.
3. Initial channel area, fluid density, and fluid velocity are used to set the mass flow rate, which from the mass conservation derivation is known to be constant throughout the channel.
4. Momentum and Energy equations are integrated as:

$$\dot{m} = \rho u A_c = \text{constant} = C_1$$

$$dP = \left( -\frac{C_1}{A_c} \frac{du}{dx} - \frac{P}{A_c} \frac{dA_c}{dx} - \frac{\tau_w C}{A_c} \right) dx$$

$$dh = \left( \frac{dq}{dx} - \frac{u du}{dx} \right) dx$$

With acceleration and area variation being found explicitly, and heating and friction being kept constant throughout.

5. The updated fluid properties are then fed back through Clausius II in order to obtain the rest of the fluid properties and update terms in the integrals.
6. Repeat steps 4) and 5) as required.

---

<sup>2</sup>The momentum conservation equation derived was found to be incorrect in Kee, the explanation and correction is shown in Chapter 9. The equation was corrected and the results were updated in Chapter 9

The approach outlined above uses a first-order forward-stepping explicit scheme in order to solve the conservation equations. Although implicit schemes were initially considered, the Clausius II property update had to be done explicitly. This limited the method approach and resulted in the fully explicit scheme developed. In order to check that the level of accuracy was being preserved through simulations, a convergence study was ran on various step sizes.

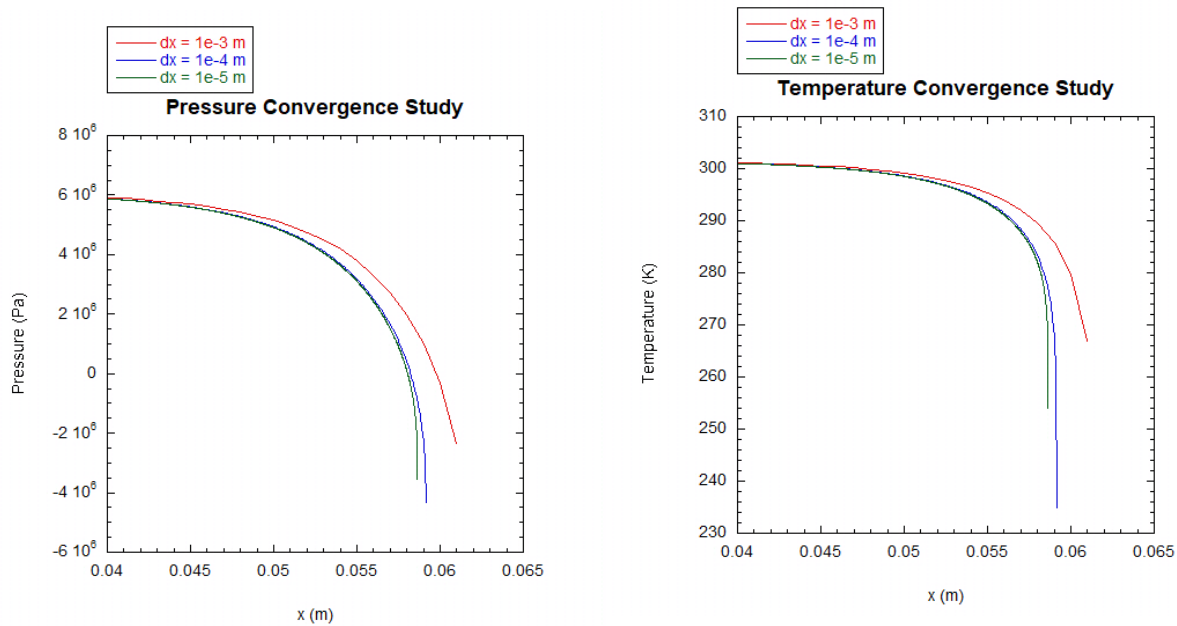


Figure 21: Convergence Study

What was seen was that the trends exhibited by the changing step sizes converged to the same values at the same point in space, thus giving credibility to the method used. What this was attempting to illustrate, was that the results obtained weren't simply a product of the step size, but actually solving the equations. A comparison study was also tested to compare the time consumption of each case.

In order to preserve accuracy while also limiting the runtime of the simulations, a step of  $1e-4$  m was chosen. Though faith is help in this approach and these results, future work will expand into

<b>Step Size (m)</b>	<b>Total Steps</b>	<b>Duration of run (s)</b>
1e-3	60	192.8
1e-4	591	2515.9
1e-5	5863	19317.1

higher-order stepping and implicit schemes. As the present code exists, it is able to sufficiently capture flow effects in order to be valid for the results and conclusions presented.

The initial conditions used in the simulations were based on realistic values for cold flows of nitrous oxide, though variations on the initial conditions were used in order to test fluids closer to critical conditions or saturation conditions. The use of a constant heat addition was incorporated as a varied heat addition condition was not known, nor were realistic values. This led to a broad range of values being used in order to capture the effects resulting from heat addition to the simulation. The value for the friction terms were based on documented data for nitrous oxide, though some variation was tested in order to account for a rougher wall increasing the effects from friction.

The final code was able to step through a one-dimensional channel explicitly while updating fluid properties based on the Clausius II equation of state.

CHAPTER VII  
EQUATION OF STATE COMPARISON

Previous formulations of Fanno and Rayleigh flows have utilized the ideal gas law in order to obtain theoretical models for varied Mach. In the case being researched, the fluid in question began as a pure liquid, thus negating the relation established in the ideal gas law. In order to demonstrate the large difference between the Ideal Gas Law and Clausius II, the formulation use in [20] was applied to Clausius II. The plots below demonstrate the significant difference found using the more appropriate Clausius II model.

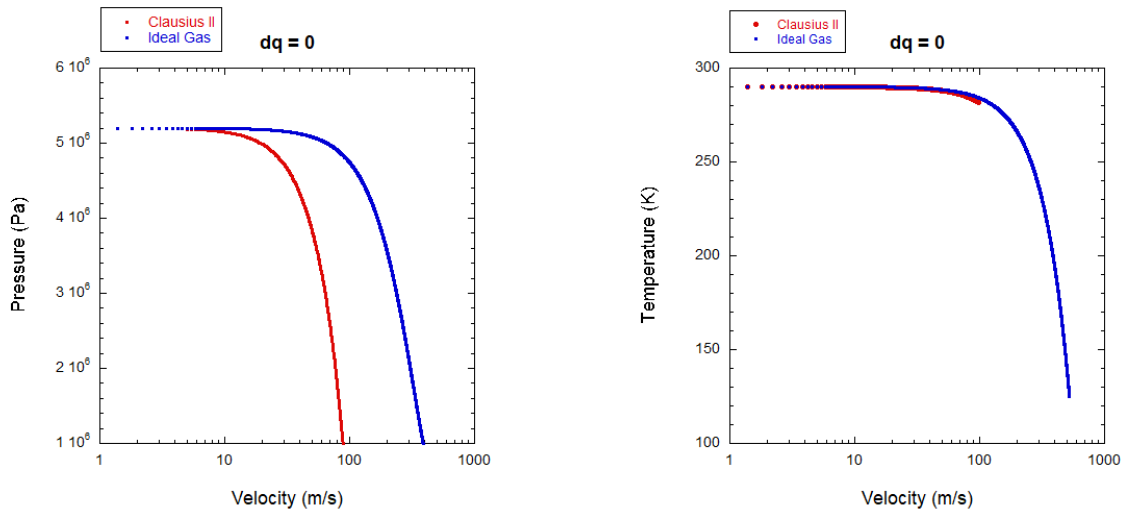


Figure 22: Clausius II vs Ideal Gas

While generating this data, it was seen as trivial to demonstrate the effects of a constant  $dq/dx$  on these plots. This in turn provides velocity dependent Rayleigh plots.

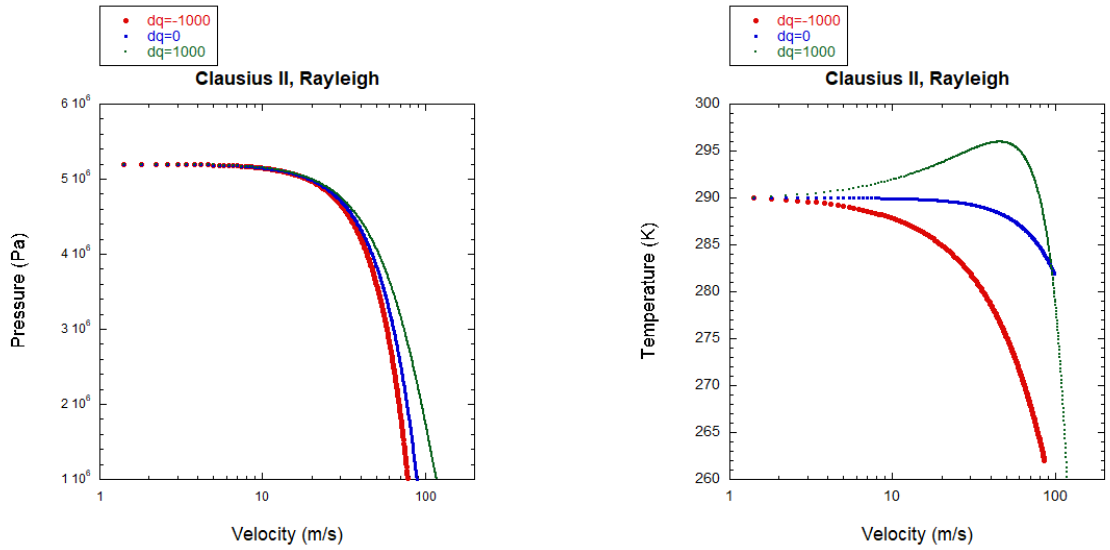


Figure 23: Clausius II vs Ideal Gas

The resulting data allows us to clearly see that the equation of state applied to the system has a significant impact on the results. They also demonstrate that heating and cooling of a system is able to vary the results.



CHAPTER VIII  
SIMULATION RESULTS

Multiple runs of the developed code were run with varying conditions of heating, friction, and area. The trends observed are reported below.

**Fanno**

In order to isolate the effects from friction in this simulation, the heating variable and the  $\frac{dA}{dx}$  term were both set to zero. This left the friction term as the only variable input in the code aside from initial conditions. The equations to be used become:

$$\dot{m} = \rho u A_c = \text{constant} = C_1$$

$$dP = \left( -\frac{C_1}{A_c} \frac{du}{dx} - \frac{\tau_w C}{A_c} \right) dx$$

$$dh = \left( -\frac{u du}{dx} \right) dx$$

The friction factor,  $f$  is accounted for in the wall shear,  $\tau_w$ , as:

$$\tau_w = \frac{\rho u^2}{2} f$$

$$f = \frac{16}{Re}$$

$$Re = \frac{\rho u D}{\mu}$$

The friction term to Reynolds number relation used is based on a laminar flow analytic solution for cylindrical tubes [19]. The  $\mu$  term used represents the dynamic viscosity of the fluid was found online for N2O, though variation on it will be considered. Variation on the friction term correlates

to the consideration of a rougher or smoother internal pipe lining.

## Results

Setting a range of initial pressures and temperatures, a series of simulation were run under varying friction factors with a constant mass flow rate.

Initial Conditions:

- Initial Pressure: [5.2 MPa, 7.24 MPa]
- Initial Temperature: [290 K, 309 K]
- Fluid: N<sub>2</sub>O
- Chamber Geometry: Constant 11.467mm Radius
- Mass Flow Rate: 1 kg/s

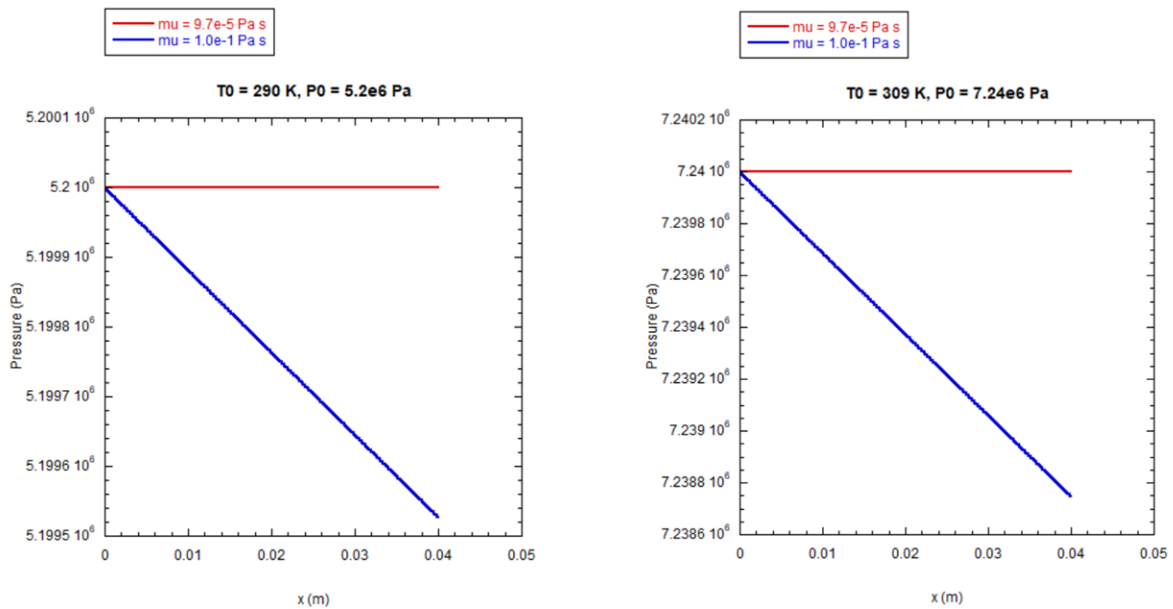


Figure 24: Fanno Results

As would be expected from the momentum equation formulation, the constant wall shear results in a close to linear reaction by the pressure term in the flow; furthermore, increasing the wall shear through the friction factor results in an increased effect on pressure.

For a realistic friction term, the flows showed minimal variance through the channel. For a value of dynamic viscosity 4 orders of magnitude higher than that expected, the effects are still quite small on the fluid properties. The results from these simulations point to friction effects not being large enough to illicit a metastable response in the system. It should be noted that this conclusion is valid for the channel dimensions being looked at, around 40 cm, longer channels may have a higher effect from friction; however, that is not relevant to the present work.

## Rayleigh

In order to isolate the effects from heating in this simulation, the wall shear and the  $\frac{dA}{dx}$  term were both set to zero. This left the heating term as the only variable input in the code aside from initial conditions. The equations to be used become:

$$\dot{m} = \rho u A_c = \text{constant} = C_1$$

$$dP = \left( -\frac{C_1}{A_c} \frac{du}{dx} \right) dx$$

$$dh = \left( \frac{dq}{dx} - \frac{u du}{dx} \right) dx$$

## Results

Setting a range of initial pressures and temperatures, a series of simulation were run under varying external heating with a constant mass flow rate.

Initial Conditions:

- Initial Pressure: [5.2 MPa, 7.24 MPa]

- Initial Temperature: [290 K, 309 K]
- Fluid: N<sub>2</sub>O
- Chamber Geometry: Constant 11.467mm Radius
- Mass Flow Rate: 1 kg/s

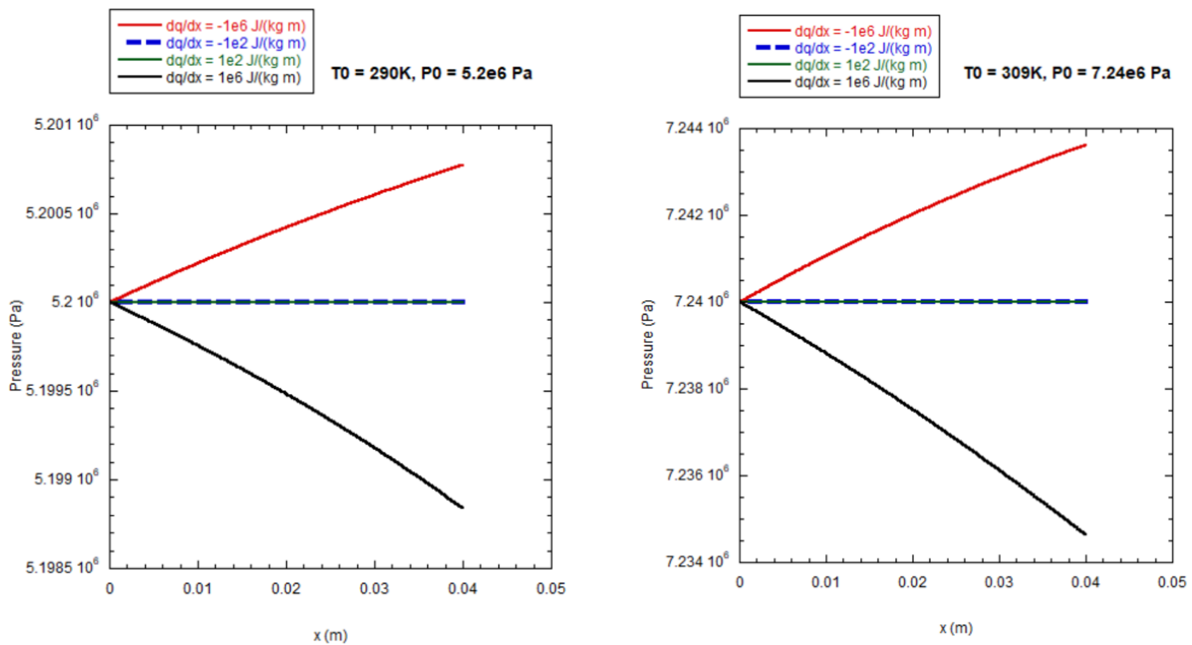


Figure 25: Rayleigh Results

The results from these simulations show that the heating and cooling of the system has a more notable effect on the pressure through the channel once the values are large enough. The results still do not show enough effect on the properties to illicit metastable behavior, but the effects are larger than those seen in the Fanno flow simulations.

### Area Variation Based on Kee

In order to isolate the effects from area variation in this simulation, the wall shear and the heating terms were both set to zero. This left the area variation term as the only variable input in the code

aside from initial conditions. The equations to be used become:

$$\dot{m} = \rho u A_{c0} = \text{constant} = C_1$$

$$dP = \left( -\frac{C_1}{A_{c,previous}} \frac{du}{dx} - \frac{P}{A_c} \frac{dA_c}{dx} \right) dx$$

$$dh = \left( -\frac{u du}{dx} \right) dx$$

## Tank Geometry

Among the cases of tank explosions discussed in Chapter 3 was the explosion of a Nitrous Oxide tank at Texas A&M during an Aero 402 class which was presented in Chapter 4. The ruptured tank was collected and was accessible during the work presented. As such, a portion of the tank was used to create a geometry profile to implement in the code.

To begin, pictures of the fractured tank were taken. The pictures of the inner contour were then converted to PDF and traced by the "Data thief" JAVA program. The raw data obtained from this trace was moved into Kaleidagraph, where a combination of 7th order polynomial fits were used in order to obtain a step function for  $\frac{dA}{dx}$ .

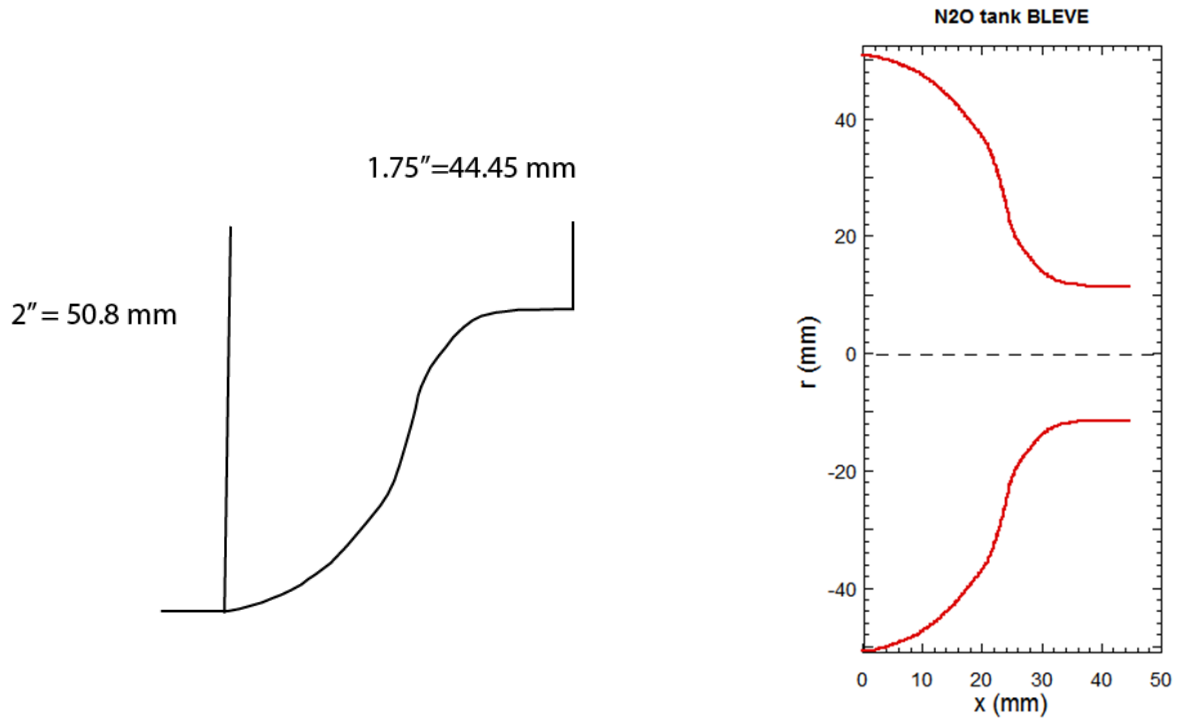


Figure 26: N2O Tank

This function was implemented into the code in order to give a realistic area variation to test with. Although the initial mentality was to go with a converging nozzle, simulations showed an increasing pressure value, thus going away from Saturation conditions and the zone for metastability. This combined with the rupture happening within the tank, led the simulation to focus on diverging nozzle conditions. Additionally to the tank geometry, the idea to include some form of recirculation was followed. As such, an exponential power nozzle interior was generated and used as a second area variation geometry.

## Results

Simply under the effects of the area variation, the effects on the fluid were the most apparent out of the effects being tested. Setting a range of initial pressures and temperatures, a series of simulation were run under varying external heating with a constant mass flow rate.

Initial Conditions:

- Initial Pressure: [5.2 MPa, 7.24 MPa]
- Initial Temperature: [290 K, 309 K]
- Fluid: N<sub>2</sub>O
- Chamber Geometry: [Tank Geometry, Exponential Geometry]
- Mass Flow Rate: 1 kg/s

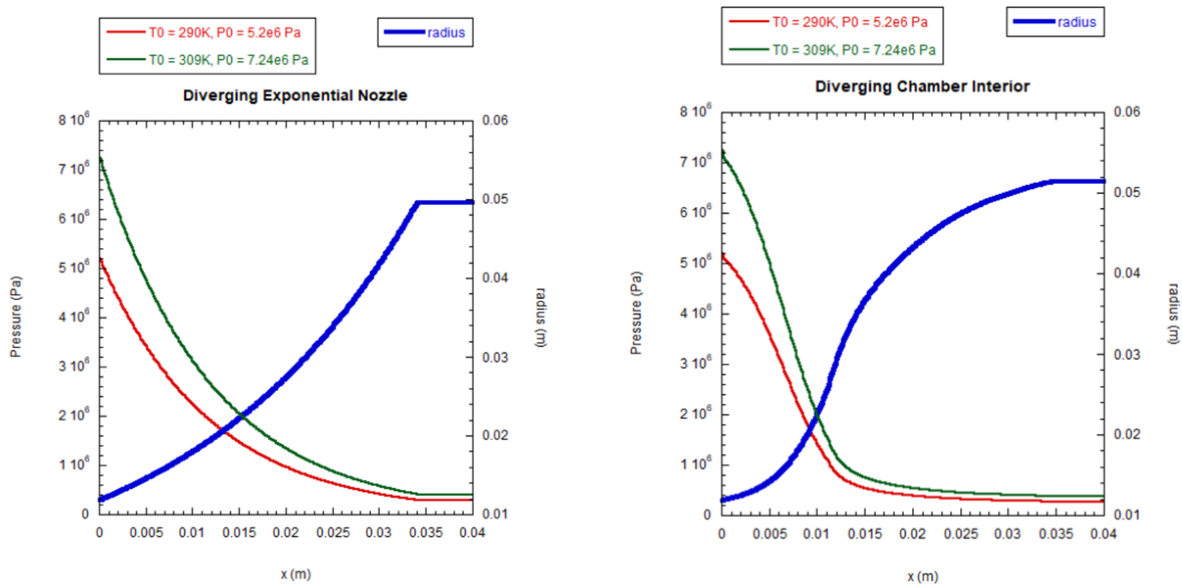


Figure 27: Area Variation Results: Pressure v X

The results obtained showed a large change in pressure, which aligns with what would be expected; however, the pressure decrease didn't show a metastable trend. In order to better analyze these results, the Pressure vs Specific Volume figures were generated

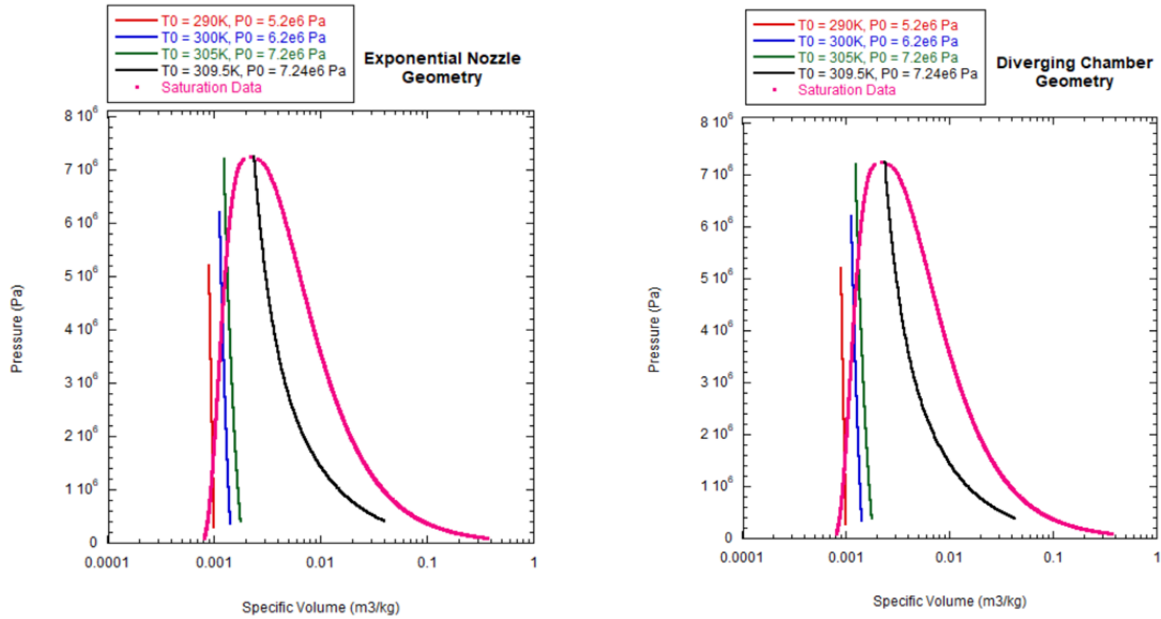


Figure 28: Area Variation Results: Pressure v Specific Volume

What was noted from the analysis of the results, was that the temperature of the fluid seemed to lower itself in order to counter the effects from the varying area in an attempt to lessen the effects on density. The results were then compared to the isotherm based on the starting temperature.

The following section, combination of effects.

### Combination of Effects

#### Rayleigh + Area Variation

Returning back to the chamber geometry depicted in section 8.3.1, simulations were run with variable heating also being employed. Setting a range of initial pressures and temperatures, a series of simulation were run under varying external heating with a constant mass flow rate.

Initial Conditions:

- Initial Pressure: [5.2 MPa, 7.24 MPa]
- Initial Temperature: [290 K, 309 K]



- Fluid:  $N_2O$
- Chamber Geometry: [Tank Geometry, Exponential Geometry]
- Mass Flow Rate: 1 kg/s

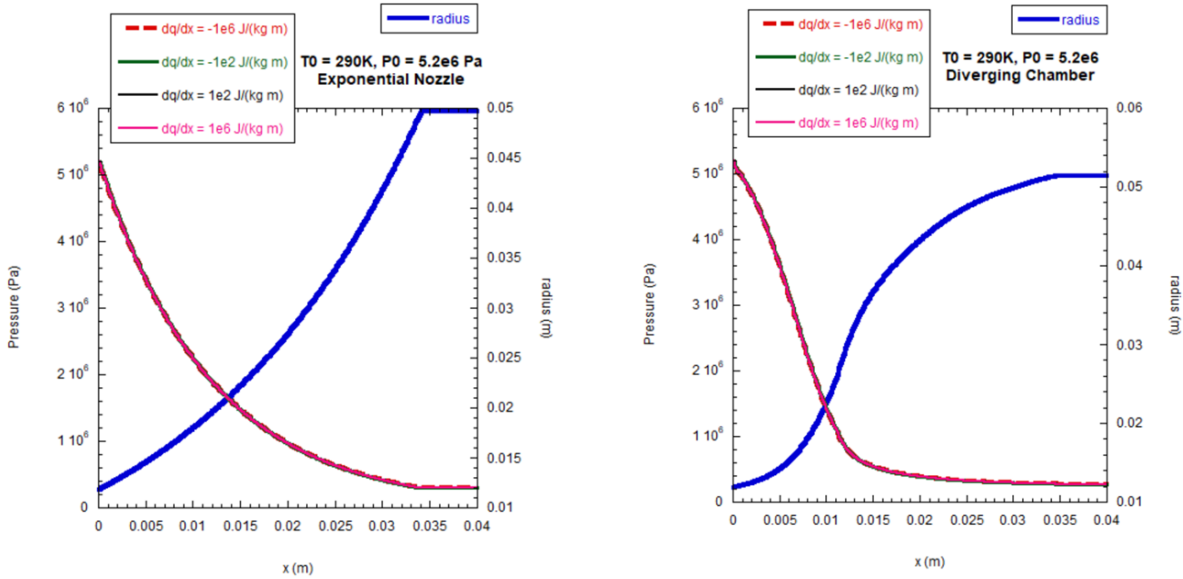


Figure 29: Rayleigh+Area Variation: Pressure vs x

From analysis of the results from a varying mass flow rate and heating, it is easy to see that the dominating factor contributing to fluid properties is the area variation. A look at the PV diagram showed something of note.

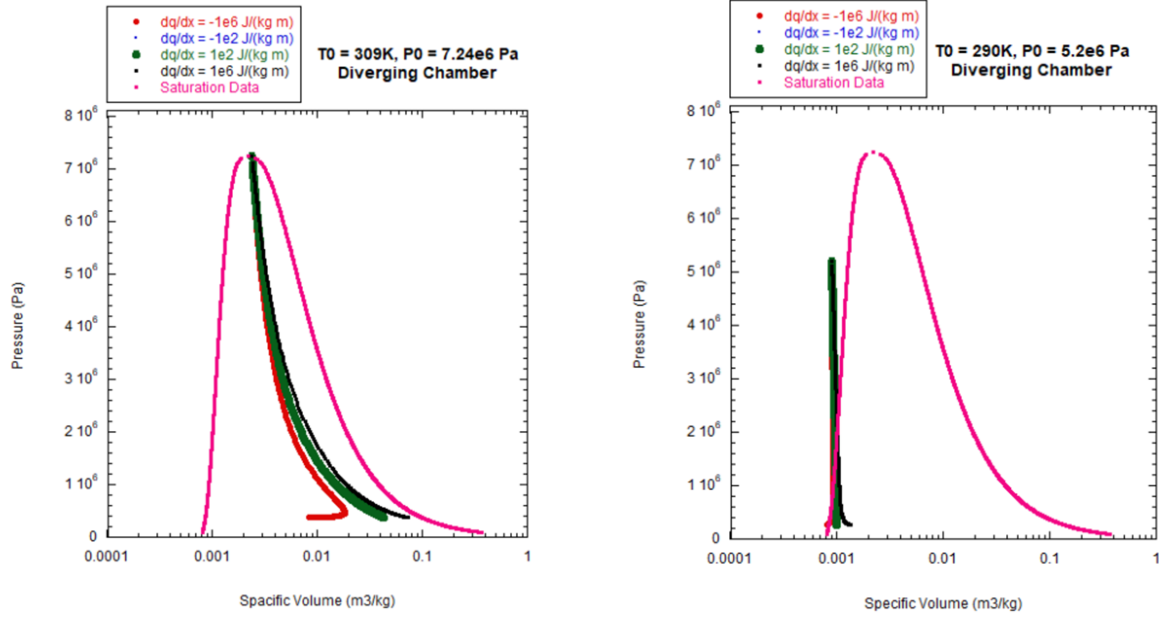


Figure 30: Rayleigh+Area Variation: Pressure vs Specific Volume

Once the values of pressure were low enough, the heating term could make itself better known. Heating of the system caused a faster decrease in density, while cooling of the system caused an increase in the density of the system.

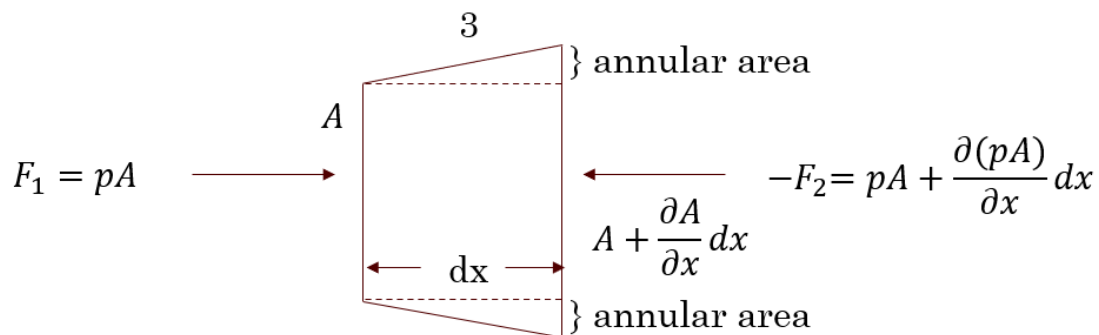
CHAPTER IX  
MOMENTUM CONSERVATION CORRECTION

**Updated Momentum Conservation Equation**

At this point, all hope seemed lost on showing metastable phase changes through adiabatic means; however, a step back was taken at what the results obtained were showing. When considering flow through a nozzle, even Bernoulli depicts a decreasing pressure for an increasing flow velocity. So was nature wrong, or was the initial derivation wrong.

An investigation was conducted into the momentum conservation derivation, as the  $P \frac{dA}{dx}$  term seemed to dominate, through order of magnitude, the other terms in the equation. What was uncovered, was another momentum derivation which eliminated this term and provided results which better aligned to what expectations based on experience predicted. The difference between the two derivations was that the derivation produced by Kee only accounted for upstream and downstream pressure force effects on the control surface, while the new derivation, obtained from George Emmanuel's Gasdynamics textbook [24], accounted for the wall pressure force effects as well.

The derivation begins with the figure depicted below [24].



As previously stated, the original derivation only considered the pressure force effects on the two perpendicular surfaces, which if added will once again give us the original momentum conservation. However, the addition of the term from the wall pressure is necessary in order to fix the equation.

$$dF_3 = \left( (p + (p + \frac{\partial p}{\partial x} dx)) / 2 \right) \left( (A + \frac{\partial A}{\partial x} dx) - A \right)$$

The simplification of this term gives us:

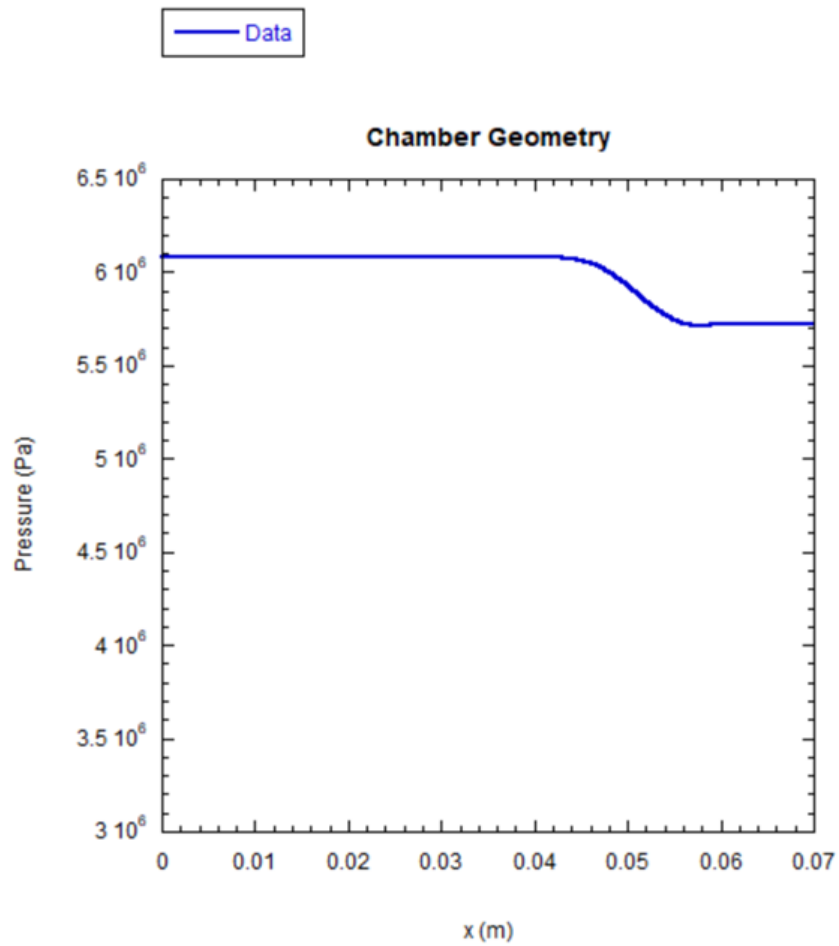
$$dF_3 = p \frac{\partial A}{\partial x} dx$$

When this force term is added to the other two terms, the momentum equation for area variation becomes:

$$\boxed{\rho u A_c \frac{du}{dx} = -A_c \frac{dP}{dx}}$$

## Updated Chamber Area Results

The updated equation was used with the chamber area in order to now correctly show the trend of a decreasing pressure with an increasing flow velocity.



Although the effects were not as large as the incorrect area variation results, this gave as a start in the right direction as the correct trend is being shown. This seems to demonstrate that channel geometry is unable to cause rapid property changes, but fluids passing through a channel will not actually stick to the geometry, as will be discussed in the next section.

## Vena Contracta

Expanding on the mindset of the exponential nozzle, the phenomenon of Vena Contracta was explored further through the extension of the chamber geometry to encompass the smaller diameter pipe fitting as well as better matching the expected effective flow through the resulting geometry.

Vena Contracta is the section in a flow where the cross-sectional area of the effective stream is at its minimum. This doesn't occur exactly at the orifice position, it is found to occur further downstream and at a lower diameter than the orifice itself. Vena Contracta is caused as a result of fluid streams being unable to abruptly change their directions, instead the streamlines follow more gradual curves along sharp geometry variations [31]. These gradual curves extend through the orifice and result in continued contraction up to a point. This point is dubbed the point of Vena contracta. Beyond this point, the effective flow returns to fill the channel geometry as shown in Figure 31.

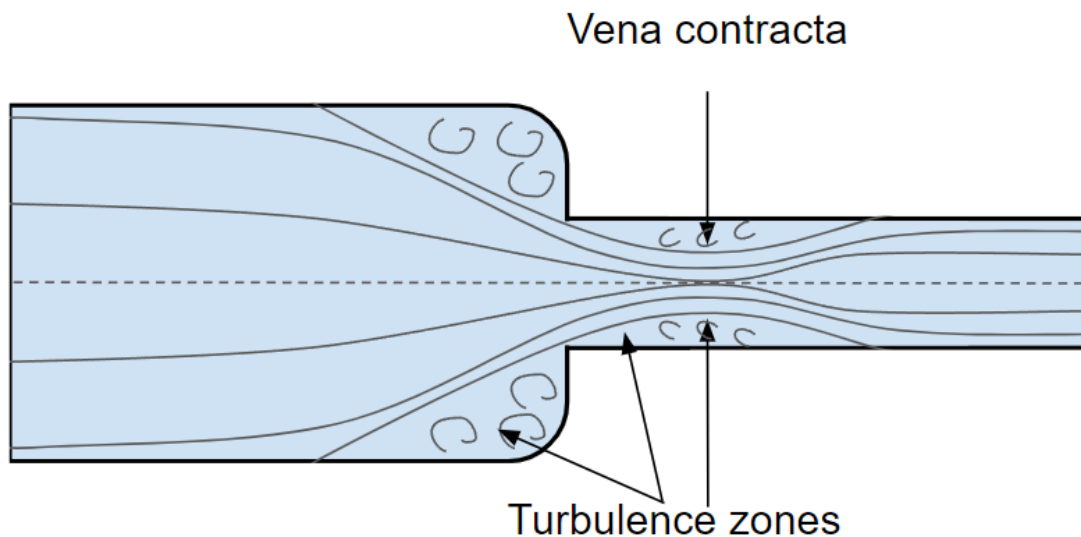
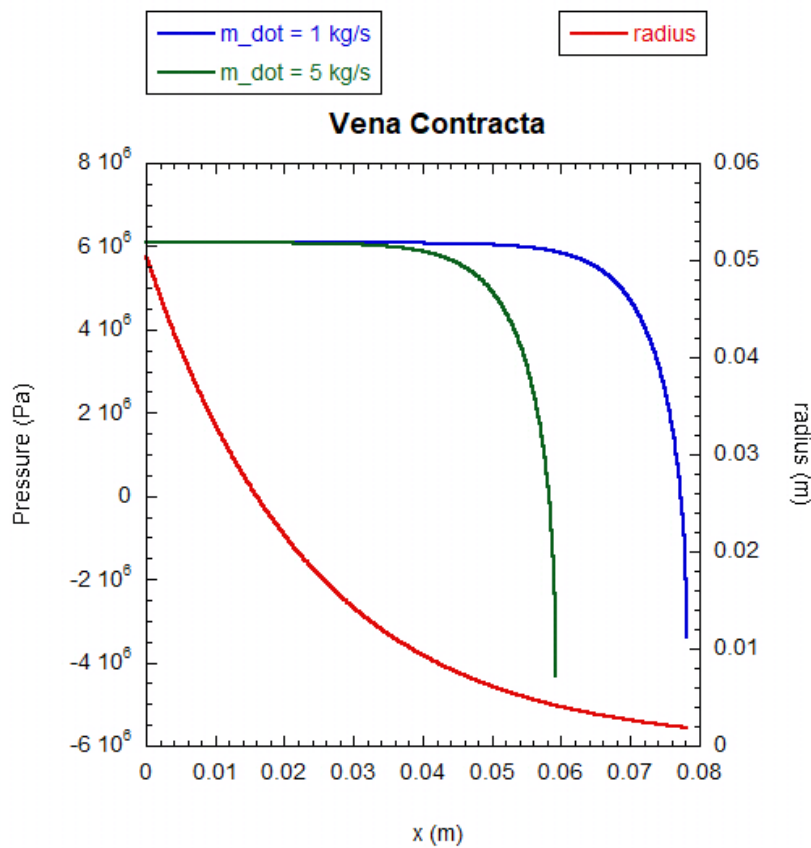


Figure 31: Vena Contracta  
(Modified from [28])

Through the application of Vena contracta, the new flow geometry produced was based on the extended exponential nozzle. The extension of the exponential nozzle geometry was finally able to produce results which demonstrated rapid property variations through a nitrous oxide flow without requiring heating to do so.

### Updated Exponential Nozzle Results

The corrected momentum conservation equation was used in combination with an extended exponential effective flow geometry in order to produce the following results of area variation on a flow. These results had no effects from friction nor heating.



What these results demonstrate, is a rapid pressure change in a fluid without the addition of heating, which gives credence to the idea being investigated of an adiabatic metastable phase change. The

fault in the data, is that the phase seems to be caught and unable to be kicked to the actual phase transition which would be expected under such rapidly changing conditions. The idea put forth is that a transient term needs to be incorporated into the simulation in order to allow a reaction by the upstream pressure to the pressure dive which could lead to the kick needed for the phase change to occur. The rapid pressure drop is allowed to occur by the model formulation without any metastable behavior as a result of temperature not being held constant. The variation of temperature prevents the flow properties from following an isotherm, instead passing through many.

Future work will need to expand on the obtained results by accounting for the transient effects through the flow. Such a rapid pressure change will cause effects to travel upstream, which will change the flow and possibly give the kick required for the metastable phase change to occur.



## CHAPTER X

### SUMMARY AND CONCLUSIONS

#### **Conclusion**

A cubic equation of state, Clausius II, was used to derive the equilibrium thermodynamic properties of N<sub>2</sub>O and coded into a usable model. Analysis of the qualitative results from the coded model were compared to expected trends in order to verify that the model is working correctly. The resulting thermostatic model was used to reproduce a plot produced by Reid which provided a thermostatic theory for conditions which could lead to metastable phase changes adiabatically.

A one-dimensional simulation through space was used in order to attempt to demonstrate metastable trends through a flow; however, though large pressure changes were noted, the phase change was not observable in the results from the simulations. The simulations run were focused on three major factors which were theorized to possibly cause metastability trends to arise through the flow. The three factors were friction (Fanno flow), external heating (Rayleigh flow), and area variation through the channel. Though friction showed minimal effects in the flow, area variation and heating did cause notable effects on the flow. Combinations of effects were also analyzed.

The one-dimensional simulations were unable to capture metastable phase changes, though the results obtained did not discredit the theory. The results instead pointed to the need of more dimensions in order to better capture the flow effects on fluid properties. The results also aided in showing a fault incorporated in some textbooks such as [19] which result in an incorrect momentum conservation equation. The mistake was traced back to incorrectly accounting for pressure force effects on the system, causing a high order term to remain, which would dominate all other effects and result in unphysical results. The corrected equation was used in order to obtain results which demonstrated rapid property changes without heat addition.

Effective flow geometry was used in combination with a recovered exploded tank's geometry, and

the effect of Vena contracta in order to formulate a geometry to test adiabatic flow conditions with area variation. This area variation was used in order to produce the results previously discussed, which demonstrated rapid property variations under adiabatic conditions.

### **Future Work**

A topic of discussion is the addition of time as a dimension in the simulation. Future work will look into how the noted pressure changes affect the upstream flow as a function of time, which may in turn capture metastable trends.

A second order term will also be added to the momentum conservation in order to capture discontinuities resulting from shocks in the flow.

## BIBLIOGRAPHY

- [1] NFPA 921 Guide to Fire and Explosion Investigations 2021 Edition. National Fire Protection Association. Page 251
- [2] Emanuel, G., "Advanced Classical Thermodynamics," AIAA Educational Series, Washington D.C., 1987, pp. 15-52
- [3] Brown, P. N., Byrne, G. D., & Hindmarsh, A. C. (1989). VODE: A variable-coefficient ODE solver. Society for Industrial and Applied Mathematics. *SIAM Journal on Scientific and Statistical Computing*, 10(5), 1038-14. doi:<http://dx.doi.org/10.1137/0910062>
- [4] Karpetis, A. "Miniature Supersonic Burner for the Study of Combustion at Extreme Conditions. II: External Flow," *Journal of Energy Engineering*, doi:10.1061/(ASCE)EY.1943-7897.0000574
- [5] McElrath, J., Karpetis, A., "Generation of Metastable Trends Through the Implementation of the Clausius-II Equation of State"
- [6] Debenedetti, P.G., "Metastable Liquids: Concepts and Principles," Introduction: Metastable Liquids in Nature and Technology/Thermodynamics, Princeton University Press, Princeton, 1996, pp. 1-146
- [7] Maxwell, J., "On the Dynamical Evidence of the Molecular Constitution of Bodies," *Nature*, March 4 1875, pp. 357-359
- [8] Bailbar, S., and Caupin F., "Metastable Liquids," *Journal of Physics: Condensed Matter*, Vol. 15, No. 1, 2002, pp. S75-S82, doi: 10.1088/0953-8984/15/1/308
- [9] Davitt, K., Rolley, E., Caupin, F., Arvengas, A., and Bailbar, S., "Equation of state of water under negative pressure," *Journal of Chemical Physics*, published online 2 Nov. 2010, doi: 10.1063/1.3495971

- [10] Reid, R.C., "Possible Mechanism for Pressurized-Liquid Tank Explosions or BLEVE's," *Science*, 203, pp. 1263-1265, 1979
- [11] Hecht, J., "Report leaves Scaled Composites blast a mystery," *New Scientist*, published 7 February 2008, <https://www.newscientist.com/article/dn13292-report-leaves-scaled-composites-blast-a-mystery/>, last assessed 28 February 2019
- [12] Karabeyoglu A., Dyer J., Stevens, J., and Cantwell, B., "Modeling of N<sub>2</sub>O Decomposition Events," AIAA paper 2008-4933, presented at the 44th AIAA/ASME/SAE/ASEE Joint Propulsion Conference & Exhibit, 21 - 23 July 2008, Hartford, CT
- [13] White, F., "Viscous Fluid Flow," Second Edition, 1991, pp. 59-100
- [14] White, F., "Fluid Mechanics," Fifth Edition
- [15] Shapiro H. and Moran M., "Fundamentals of Engineering Thermodynamics," Fifth Edition, SI Units, 2006
- [16] Sutton G. and Biblarz O., "Rocket Propulsion Elements," Seventh Edition
- [17] Thompson, P., "A Fundamental Derivative in Gasdynamics," *Physics of Fluids* (1958-1988) 14, 1843 (1971); doi: 10.1063/1.1693693
- [18] Zucker R. and Biblarz O., "Fundamentals of Gas Dynamics," 2002
- [19] Kee R., Coltrin M., and Garborg P., "Chemically Reacting Flow"
- [20] Hill P. and Peterson C., "Mechanics and Thermodynamics of Propulsion," Second Edition
- [21] Cizmas P., Girimaji S., Saric W., Reed H., Donzis D., and White E., "Viscous Flows and Heat Transfer"
- [22] Report, E. S. (2020, July 23). Report: Nitrogen Tank was modified. *The Eagle*. Retrieved April 11, 2022, from [https://theeagle.com/news/a\\_m/report-nitrogen-tank-was-modified/article\\_8cba5186-a3a8-5a47-9e54-c2a77f55481a.html](https://theeagle.com/news/a_m/report-nitrogen-tank-was-modified/article_8cba5186-a3a8-5a47-9e54-c2a77f55481a.html)

- [23] State Fire Marshal's Alert, "University Campus Liquid Nitrogen Cylinder Explosion," 22 February 2006
- [24] Emanuel, G., "Gasdynamics: Theory and Application," AIAA Educational Series, 1986, pp. 28-29
- [25] Haase, Mateusz Wodtke, Michał. (2017). Numerical Analysis and Design of Hydrostatic Thrust Bearing for the Laboratory Test Rig. 10.13140/RG.2.2.14715.00800.
- [26] National Institute of Standards and Technology. (n.d.). Saturation properties for dinitrogen monoxide. Saturation Properties for Dinitrogen monoxide. Retrieved June 6, 2022, from <https://webbook.nist.gov/cgi/fluid.cgi?Action=Load&ID=C10024972&Type=SatP&Digits=5&THigh=309.52&TLow=182.33&TInc=0.1&RefState=DEF&TUnit=K&PUnit=MPa&DUnit=mol%2Fl&HUnit=kJ%2Fmol&WUnit=m%2Fs&VisUnit=uPa%2As&STUnit=N%2Fm>
- [27] "Modeling of N<sub>2</sub>O Decomposition Events", M.A. Karabeyoglu, J. Dyer, J. Stevens and B. Cantwell, AIAA-2008-4933, AIAA/ASME/SAE/ASEE Joint Propulsion Conference and Exhibit, Hartford, CT, July 21-23,2008
- [28] Haase, Mateusz Wodtke, Michał. (2017). Numerical Analysis and Design of Hydrostatic Thrust Bearing for the Laboratory Test Rig. 10.13140/RG.2.2.14715.00800.
- [29] Pourkarimi, Ziaeddin, Bahram Rezai, and Mohammad Noaparast. "Effective parameters on generation of nanobubbles by cavitation method for froth flotation applications". *Physicochemical Problems of Mineral Processing* 53 no. 2 (2017): 920-942. doi:10.5277/ppmp170220.
- [30] Robert T. Balmer, "Modern Engineering Thermodynamics", Chapter 16 - Compressible Fluid Flow, Academic Press, 2011, Pages 651-691, <https://doi.org/10.1016/B978-0-12-374996-3.00016-6>.

- [31] Mecholic. (n.d.). What is Vena contracta? how vena contracta formed in fluid flow? Mecholic. Retrieved June 9, 2022, from <https://www.mecholic.com/2018/11/what-is-vena-contracta.html>
- [32] Sethna, J. P. (2007). 11.3 Nucleation: Critical Droplet Theory. In *Statistical mechanics: Entropy, order parameters, and complexity* (pp. 326–328). essay, Oxford Univ. Press.
- [33] Surface tension and water completed. *Surface Tension and Water* | U.S. Geological Survey. (n.d.). Retrieved June 13, 2022, from <https://www.usgs.gov/special-topics/water-science-school/science/surface-tension-and-water>